

UCSF

UC San Francisco Electronic Theses and Dissertations

Title

Regulation and function of transcription factor MEF2C in vascular development

Permalink

<https://escholarship.org/uc/item/9sh9x1tt>

Author

Anderson, Joshua

Publication Date

2005

Peer reviewed|Thesis/dissertation

Regulation and Function of Transcription Factor MEF2C in Vascular Development

by

Joshua Anderson

DISSERTATION

Submitted in partial satisfaction of the requirements for the degree of

DOCTOR OF PHILOSOPHY

in

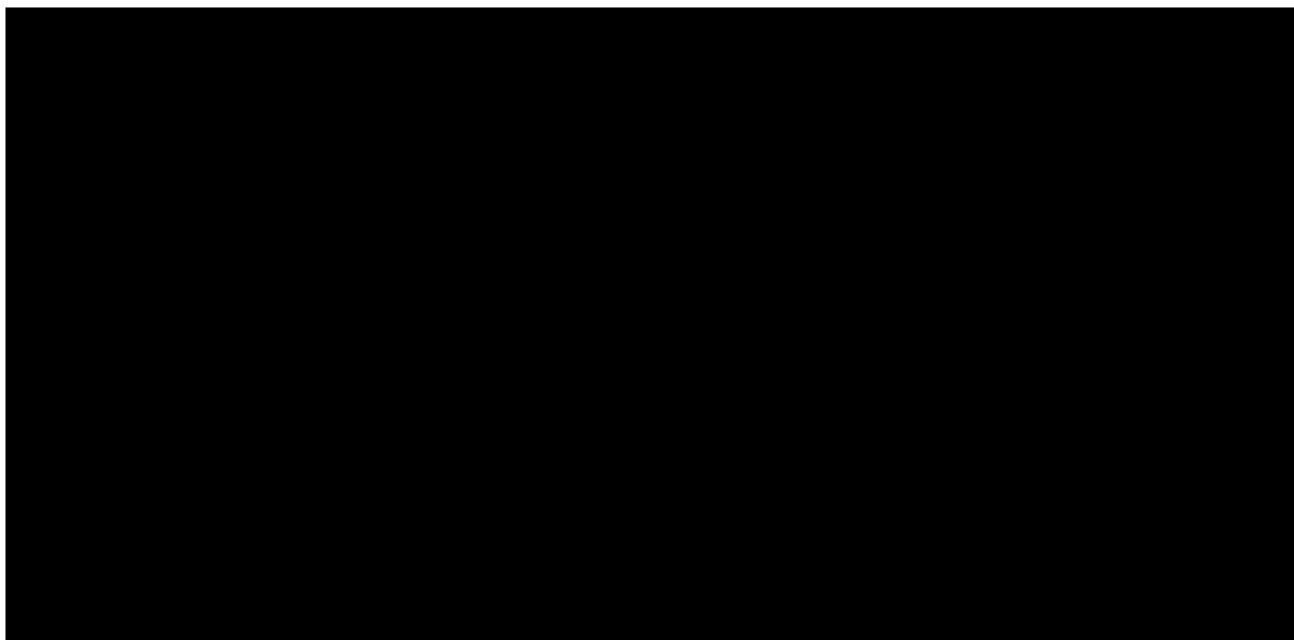
Biomedical Sciences

in the

GRADUATE DIVISION

of the

UNIVERSITY OF CALIFORNIA, SAN FRANCISCO



Copyright (2005)

by

Joshua Anderson

Dedicated to my children: Nicholas and Stephen

I am so proud of both of you

Acknowledgements

I want to thank everyone who has helped me along the way during this long journey toward my degree. Graduate school has definitely been the toughest challenge that I have faced and I couldn't have made it through without the help of so many people who I wish to acknowledge here.

First, I want to thank my mentor, Brian Black for all that he has done for me and taught me. Brian took me into his lab and gave me guidance when I needed it most and has continued to be such a great teacher throughout my graduate studies. I really appreciate all of the opportunities that he has provided for me. He has always been there for me whether it has been to listen to a practice talk or help me through a scientific problem, and he definitely takes his role as graduate advisor seriously. But probably most importantly, his advice and candor have helped me grow as a scientist and as a person and I thank him for that.

I also want to thank all of the members of the Black Lab past and present for all of their help and support over the years. Evie's work in the lab laid the foundation upon which most of my work was built on and I thank her for her help getting my projects started. Stephanie and Eric have spent countless hours in a smelly mouse room to take care of, cross, genotype, and keep track of all of my mice. Anabel, Sarah, and Jae-Yeong have provided much good advice about science, experiments, and life in general. And finally, my fellow graduate students: Eric, Analaeah, Mike, and Dustin who have experienced this journey with me, offering their help and expertise when needed and often reporting back with the locations of free cookies, happy hours, and seminars with free food. Everyone in the lab has shared many things with me including parenting

advice, barbecues, beer, sporting events, soccer games, aluminum foil, and of course some lively discussions that have covered the gamut from Mother Teresa to Hitler, and sometimes compared the two, well almost.

The last four years have been very exciting and prosperous for me, but there were times during my graduate career when things were not going well and I want to thank Zena, Krystyna, Sergei, Yong Ping, Charlie, Max, Valeria, Petros, Bryony, Eleni, and Steffi for their help through the tough times. I especially want to thank Larisa and Patrick who were always there for me when times were tough and I needed a lot of advice and encouragement.

I also want to thank my committee for their advice and guidance throughout my graduate career. Holly Ingraham has been a great committee chair. Throughout my graduate career she has always been supportive of me and interested in what I was doing. As a committee chair, she made sure that my project was going in the right direction and that I had a backup plan in case it didn't work. Rong Wang also has been very supportive of my work, and me as well. As the committee member with the research interests most similar to mine, she was a very good source of scientific ideas, information, and career advice. And finally, I owe a great debt to Zena Werb, who other than Brian, has been the faculty member that has had the greatest influence on me at UCSF. I met Zena my first day at UCSF because she was assigned to be my faculty advisor. That day she told me to think of her as my Jewish mother at UCSF and that she was there to look after me and help me with any problems that I might encounter. Zena certainly lived up to her promise. In addition to serving on my dissertation committee, she was also on my orals committee and was always willing to take the time to sit down with me and offer advice

whenever I needed it. She has been there for me from start to finish and I am very grateful for her help.

And last, but not least, I want to thank my family for all that they have done for me. First of all, I especially want to thank my parents: John and Kathleen, and my grandparents: Bruce, Pearl, Martin, and Marion; not only for bringing me into the world, but also for instilling in me, by their examples, the importance of education and integrity. Without their love and support, I could not be where I am today. I also want to thank my brother Peter and sister Mollie for their support and their help over the years honing my debating skills. In addition to my own parents, I have been especially blessed to have wonderful in-laws in Larry and Caryn who are extremely supportive and always happy to help watch the grandchildren. Speaking of which, I thank my children, Stephen and Nicholas for the hugs and smiles and laughter around the house that put everything into perspective for me. And finally, I want to thank my wonderful wife Laurie for everything that she has done for me. She has listened to my problems, accepted the strange hours that science sometimes demands, given me two extraordinary children (at the same time no less!) and throughout it all, been amazingly supportive. Without her as my wife, I don't know what I'd do.

The figures in Chapter 2 are exact copies of figures that appear in *Molecular and Cellular Biology*, 24:3757-3768, 2004. This article was published by Joshua P. Anderson, Evdokia Dodou, Analeah B. Heidt, Sarah J. De Val, Eric J. Jaehnig, Stephanie B. Greene, Eric N. Olson, and Brian L. Black.

Regulation and Function of Transcription Factor MEF2C in Vascular Development

Joshua Anderson

Abstract

Blood vessel development in vertebrates starts early during embryogenesis with the *de novo* formation of blood vessels through the process of vasculogenesis. During vasculogenesis, endothelial progenitor cells coalesce into tubular structures. Pericytes and smooth muscle cells then surround these tubes to form functioning blood vessels. Myocyte enhancer factor 2 (MEF2) transcription factors have been shown to play a critical role in the differentiation of cardiac and skeletal muscle. MEF2C is also expressed in several other cell types, including smooth muscle and endothelial cells, yet little is known about the transcriptional pathways in which MEF2C participates, particularly during vascular development.

Before the research contained within this dissertation, no transcriptional targets of MEF2 proteins had been discovered in smooth muscle. However, we found a completely conserved MEF2 site upstream of the *HRC* transcriptional start site that proved to be necessary for expression of a *lacZ* transgene in skeletal, cardiac, and arterial smooth

muscle; identifying *HRC* as the first known target gene of MEF2 in smooth muscle. We also found that this *HRC* enhancer was unresponsive to serum response factor (SRF), making *HRC* one of only a few smooth muscle genes known not to be a transcriptional target of SRF.

To understand the transcriptional pathways that MEF2C participates in, we initiated an enhancer screen and used evolutionary conservation to identify multiple tissue-specific modular enhancers for *mef2c*. In this screen, we identified a skeletal muscle enhancer, an anterior heart field enhancer, three neural crest enhancers, and two endothelial enhancers at the *mef2c* locus. One of the enhancer fragments we discovered was a 5.6 Kb fragment that is sufficient to direct expression to both the neural crest and endothelium. We have subsequently separated the neural crest and endothelial elements into two independent enhancers and pared down the endothelial element to a mere 44 base pairs, which are both necessary and sufficient to direct expression of the *lacZ* reporter to endothelial cells. Within this 44 bp we have found two ETS factor binding sites and an E-Box that are necessary for endothelial expression, and we continue to search for other regulatory elements.


Brian Black, Thesis Advisor

Table of Contents

Chapter 1 - Introduction	1
Chapter 2 - MEF2-Dependent Regulation of <i>HRC</i>	13
Chapter 3 - Evolutionary Conservation of Regulatory Elements of <i>Mef2c</i>	41
Chapter 4 - MEF2C Expression in Endothelium is Directed by a 44 bp Enhancer	53
Chapter 5 — Future Directions	81
Materials and Methods	88
Bibliography	98

List of Figures

Chapter 2

Figure 1 - <i>HRC</i> Promoter and Enhancer Activity in Myoblasts and Myotubes	27
Figure 2 - <i>HRC</i> Enhancer Expression Pattern	30
Figure 3 - Deletional Analysis of the <i>HRC</i> Upstream Region	32
Figure 4 - A Conserved MEF2 Site is Found Within the <i>HRC</i> Minimal Enhancer	34
Figure 5 - The Conserved MEF2 Site is Functional in Culture and In Vitro	37
Figure 6 - The MEF2 Site is Required for <i>HRC</i> Enhancer Activity In Vivo	40

Chapter 3

Figure 7 - <i>Mef2c</i> BAC Transgenic Embryo	50
Figure 8 - Evolutionary Conservation Directs the Search for Modular Enhancers	52

Chapter 4

Figure 9 - F10 Directs Expression to Both Endothelial and Neural Crest Cells	68
Figure 10 - Evolutionary Conservation Within the 5.6 Kb F10	70
Figure 11 - Deletional Analysis of F10 Identified Two Separate Enhancers	72
Figure 12 - Schematic Representation of the 44 bp Constructs	74
Figure 13 - ETS-1 Electrophoretic Mobility Shift Assays	76
Figure 14 - The <i>Mef2c</i> Endothelial Enhancer Contains Necessary ETS and bHLH Binding Sites	78
Figure 15 - Schematic Representations of the 44 bp Constructs	80

List of Tables

Table 1 — Primer Sequences	95
Table 2 — 44 bp Oligonucleotide Sequences	96
Table 3 — Mutant and EMSA Sequences	97

Chapter 1

Introduction

The Cardiovascular System

The cardiovascular system of vertebrates serves a very basic but important purpose. This purpose is to provide oxygen and nutrients to every cell in the organism. In mammals, this requires a very complicated and extensive system of arteries, capillaries, and veins permeating throughout every tissue. In addition to providing every cell with oxygen and nutrients, the vascular system must also be able to return blood back from every cell to dispose of waste and CO₂ and maintain unidirectional flow. How this complicated system develops is a question that we are only starting to answer.

Because the cardiovascular system serves such a basic and important purpose, it is also a very clinically relevant organ system to study. According to the CDC, in 2002 the top three causes of death in the U.S. for individuals 25-85 years old were heart disease, malignancies, and cerebrovascular disease (stroke) respectively (1). If one takes into consideration that formation of new blood vessels (angiogenesis) is a necessary component of non-leukemia malignancies and the fact that the leading cause of death in the U.S. for children under the age of 5 years old is congenital anomalies (1), the clinical importance of cardiovascular research becomes clear.

The cardiovascular system develops very early during embryogenesis relative to other organ systems. The heart begins beating and circulating blood through a functional, but relatively simple vascular system by 9.0 days post coitum (dpc) in the mouse (2) and by the end of the fourth week of gestation in humans (3). The early development of the cardiovascular system in mammals is indicative of the necessity of this organ system long before the organism is born. Indeed, mice that lack a functional copy of one of the key vascular developmental genes such as *flt-1* or *flk-1*, die between 8.5 and 9.5 dpc (4, 5).

Vasculogenesis

There are two different and distinct processes by which blood vessels form: vasculogenesis and angiogenesis. Vasculogenesis is the *de novo* formation of the primary vascular network during embryogenesis. Before any vasculature is formed in the embryo, blood islands appear starting at 7.0 dpc in the yolk sac (4, 6). These blood islands are formed when members of the fibroblast growth factor family induce paraxial and lateral plate mesoderm to differentiate into angioblasts and hematopoietic cells (7). Vascular endothelial growth factor (VEGF) in particular, appears to play an active role in maintaining endothelial cell and angioblast differentiation (8, 9). Within the blood islands, the peripheral cells flatten and differentiate into angioblasts (endothelial precursor cells), and the internal cells differentiate into hematopoietic cells (5, 10). The differentiation of endothelial cells is apparently dependent on at least one of the VEGF receptors, VEGFR2, because disruption of the *flk-1* gene, which encodes the VEGFR2 protein, interferes with the differentiation of endothelial cells leading to death at 8.5-9.5 dpc (4).

Vasculogenesis begins in the yolk sac when angioblasts in the blood islands proliferate and coalesce with angioblasts from nearby blood islands to form a network of endothelial tubes (11, 12). These endothelial tubes then recruit mesodermal cells to differentiate into pericytes and smooth muscle cells (SMCs) and surround the endothelium to form a primitive vascular plexus in the yolk sac (13, 14). In the embryo itself, the process is similar: migratory angioblasts arising from the mesoderm aggregate to form tubes that will become the dorsal aortae, cardinal veins, and other major vessels

(11, 12, 15, 16). The endothelial tubes then recruit surrounding mesenchymal cells to differentiate into pericytes and SMCs and surround the tubes to become mature blood vessels that will become the foundation of the new vascular system (11, 13, 14, 17). Disruption of the *flt-1* gene, which encodes the receptor VEGFR1, permits differentiation of endothelial cells, but interferes with later stages of vasculogenesis, resulting in thin-walled vessels of larger than normal diameter and death at 9.0 dpc (5).

Angiogenesis

While vasculogenesis is defined as the *de novo* formation of blood vessels, angiogenesis is defined as the formation of new blood vessels from existing vasculature. Angiogenesis can occur through two processes: the sprouting of new vessels from an existing vessel, or the splitting of an existing vessel by intussusception into two or more new vessels (7). The growth of blood vessels by angiogenesis is largely driven by hypoxia, which upregulates VEGF (18, 19) due both to increased transcription mediated by hypoxia-inducible factor 1 α (HIF-1 α), and an increase in VEGF mRNA stability dependent on the 3' region of the mRNA (20). Lack of oxygen stimulates the release of angiogenic growth factors, including VEGF, through the action of transcription factors from the bHLH-PAS domain family. Two members of this family, HIF-1 α and arylhydrocarbon-receptor nuclear translocator (ARNT) form a heterodimer and stimulate the expression of angiogenic factors such as VEGF in response to hypoxia (13, 21-23). In the ARNT-deficient mouse, the primary vascular network forms, but subsequent angiogenesis is defective, leading to a lack of functional yolk sac vasculature, stunted growth, and death by 10.5 dpc (24). Since ARNT is a regulator of VEGF expression, it is

not surprising that the phenotype of ARNT-deficient mice is similar to that of heterozygous VEGF-deficient mice (8, 9). HIF-1 α -deficient mice also have a similar vascular phenotype and die at 10.5 dpc (25).

VEGF plays a central role in angiogenesis because it acts as an endothelial specific mitogen and chemoattractant (26). Interestingly, hyperoxia inhibits VEGF expression leading to regression and death of retinal vessels, which can be rescued by intravitreal injection of VEGF (27). As previously mentioned, VEGF is produced in response to hypoxia by non-endothelial cells not adequately served by the vascular system. VEGF then acts in a paracrine manner to bind to the VEGFR2 receptor on endothelial cells and triggers an angiogenic response consisting of endothelial proliferation, vascular permeability, endothelial migration, and the upregulation of a number of angiogenic genes including endothelial nitric oxide synthase (eNOS) and angiopoietin-2 (28-30). Nitric oxide is produced by eNOS and causes blood vessels to dilate. The dilated vessels then become leaky in response to the vascular permeability activity of VEGF (29).

Matrix metalloproteinases, including MMP2, MMP3 and MMP9 are activated in response to VEGF and begin to dissolve the vessel s basement membrane and surrounding extracellular matrix (ECM), clearing the way for endothelial migration into the ECM where the endothelial cells proliferate and form a new vessel, which grows into the hypoxic region (30). The receptor tyrosine kinase TIE-2 seems to play an important role in the sprouting and splitting processes of angiogenesis. In TIE-2 deficient mice, capillaries don t sprout into the neuroectoderm, yolk sac vessels are dilated and grow in

an abnormal vascular pattern, other blood vessels that should be small, show persistently large lumens, and the vessels of the myocardium fail to sufficiently branch (31).

Vascular Smooth Muscle

The initial steps of the processes of both vasculogenesis and angiogenesis consist primarily of the proliferation, migration, and tube formation by endothelial cells. However, just as important in the function of blood vessels is the recruitment of surrounding mesenchymal cells to differentiate into SMCs and surround the endothelium to provide strength, structure, and an ability to regulate blood pressure.

The signaling factors involved in vascular smooth muscle cell (VSMC) development have been fairly well-studied, and the factors that appear to play the biggest roles in differentiation of VSMCs from the mesoderm are PDGF and TGF- β (32-35). In addition, PDGF-BB and epidermal growth factor (EGF) are VSMC chemoattractants (36). However, an important question remains unresolved: which cells are recruited to differentiate into VSMCs and become a part of the vessel wall? This has proven to be a very complicated question as several different sources of VSMCs have been reported. Cells derived from the mesoderm of the neural crest have been widely reported to differentiate into VSMCs, presumably as a result of inductive signals from the endothelium (37-39). In addition, cells derived from the splanchnic mesoderm have also been reported as a source of VSMCs (40, 41). Still others, have reported that epicardial cells transdifferentiate to become coronary VSMC (33, 42, 43). And finally, there is evidence that in the dorsal aorta, some endothelial cells themselves transdifferentiate into VSMCs (44). There is evidence to support endothelial induction of SMC differentiation

of surrounding cells (33, 37-43), as well as evidence of transdifferentiation of endothelial cells themselves to become SMCs (44, 45). In summary, it appears that VSMCs can come from a variety of sources and that there is more than one developmental path a VSMC may take.

The generation of transgenic and knockout mice that are deficient in specific genes has led to several insights into the mechanisms involved in VSMC development. Angiopoietin-1 is the ligand for the TIE2 receptor, and Ang-1 deficient mice exhibit abnormal vascular architecture where the principal defect is failure to recruit SMC and pericyte precursors to nascent vessels (46). In addition, venous malformations have been mapped to the TIE2 receptor in humans. In these patients, missense mutations cause an increase in autophosphorylation of the TIE2 receptor and patients develop veins that appear to lack SMCs (14). Affected vessels in these patients have dilated serpiginous lumens with a single endothelial cell layer and thin walls with a variable smooth muscle layer, which is sometimes completely absent (14).

The transcriptional events that lead to differentiation are varied and involve many different transcription factors including SRF, Prx-1, Prx-2, CRP2/SmLIM, and members of the HOX, GATA, and MEF2 families (36). Not surprisingly, many of the genes that have been implicated in VSMC development based on mouse knockout studies are transcription factors. Targeted disruption of the Kruppel-like zinc finger transcription factor LKLF leads to vascular defects, most notably a reduction in differentiated SMCs and pericytes resulting in aneurysmal dilation of the large vessels and eventual rupture with intra-amniotic hemorrhage (47). A similar phenotype has been reported for mice lacking the cytoplasmic domain of ephrin B2, suggesting that signaling through ephrin

B2 may involve activation of LKLF or similar transcription factors during later stages of vessel development (48). Targeted disruption of the gene that encodes SMAD5, a transcription factor downstream of BMP signaling through the TGF- β receptor family (49, 50), results in apoptosis of mesenchymal cells and a marked reduction in the differentiation of mesenchymal cells into vascular smooth muscle (51). In addition, the bHLH transcription factor HAND2 has recently been shown to be crucial for yolk sac vascular development. In HAND2 null mice, endothelial cell differentiation and recruitment of surrounding mesenchymal cells occurs normally. However, the mesenchymal cells fail to differentiate into VSMCs. One of the genes that was shown to be downregulated in these mice was the VEGF₁₆₅ receptor neuropilin, suggesting that HAND2 may be a crucial mediator of the VEGF signaling pathway (52).

Transcriptional Regulation of Vascular Genes

While some transcription factors have been discovered to play a role in vascular development as a result of knockout studies, the roles of others are being discovered in studies of the transcriptional regulation of specific vascular genes. The *flk-1* gene enhancer and promoter are regulated in endothelial cells by two SCL/Tal-1 sites, a GATA site and an ETS site (53). Within the promoter of the *flt-1* gene, a cAMP response element (CRE) and an ETS site were found to regulate transcription in 293E1 cells in culture (54). Similarly, two ETS-binding sites in the *tie-2* gene appear to play a role in transcriptional regulation and are bound by the ETS family member NERF2 (55). The *tie* gene promoter contains several conserved ETS and AP-2 binding sites, mutations of most of which lead to reductions of gene expression in *lacZ* transgenic animals (56). In

addition to what we know about the transcriptional regulation of these vascular genes, we also know that targeted disruption of the gene encoding the transcription factor MEF2C results in severe vascular defects and embryonic lethality by 9.5 dpc (57, 58).

MEF2C Structure

MEF2 transcription factors belong to the family of MADS (MCM1, Agamous, Deficiens, SRF) domain transcription factors. In mice, there are four known MEF2 genes (*mef2a-d*), each one of which has several splice isoforms. The MADS domains of the MEF2 proteins mediate dimerization and DNA binding and are highly conserved between all four mouse genes as well as *mef2* genes in other species ranging from *Drosophila* to humans (59). Adjacent to the MADS domain is the MEF2 domain, a 28 amino acid motif that is also highly conserved, mediates dimerization, and is unique to the MEF2 factors (60).

Transcriptional Regulation by MEF2 Factors

MEF2 proteins act in a combinatorial fashion with other transcription factors to activate transcription of their target genes. MEF2 proteins bind to the consensus binding site: YTA(A/T)₄TAR as either homo- or heterodimers (59). In skeletal muscle, which has been studied much more extensively than either cardiac or smooth muscle, most of the transcriptional targets of MEF2 also require members of the MyoD family to act in a cooperative fashion with MEF2 proteins to activate transcription (59). MEF2 and MyoD proteins physically interact with each other and the resulting complex has a synergistic effect on their transcriptional abilities (61, 62). This synergy is made possible by the fact

that the binding sites for MEF2 and MyoD in many skeletal muscle gene promoters are found in close proximity to each other and spaced such that their binding sites are coordinately positioned on the same face of the DNA (63).

Tissue and Cell Type Expression

Mef2c is the first *mef2* gene expressed in the mouse cardiovascular system with expression evident around 7.5 dpc in cells that will eventually give rise to the heart (64). *Mef2c* expression is seen in differentiating skeletal muscle myoblasts in the rostral somites starting at about 9.0 dpc (64), and later in SMCs as these cells begin to differentiate throughout the embryo (65). *Mef2* expression is not limited to muscle cells, expression is also seen in the developing central nervous system (66, 67), lymphocytes (68), and endothelial cells (57).

Importance in Vasculature

The importance of MEF2 proteins in skeletal muscle has been appreciated for some time; however, the role that MEF2 proteins play in development of the vasculature has remained unclear. This is probably due mostly to the approaches usually taken in the field of vascular development where most of the study centers on endothelial cells (which have only recently been shown to express MEF2C). In addition, much of the current work in the vascular development field centers around the effects of growth factors and knockouts of vascular-specific genes. Coincidentally, most of our knowledge of the role of MEF2 proteins in vascular development has come as a result of the *mef2c* knockout mouse.

Mef2c null mice have severe vascular and cardiac abnormalities and die by 9.5 dpc (57, 58). Because of the severe nature of both the vascular and cardiac defects, it is difficult to assess the cause of death, and whether one of the defects is primary while the other is secondary. In any case, the vascular defects in the absence of MEF2C include the disruption of the yolk sac vasculature and either the complete lack of major blood vessels such as the cardinal veins and dorsal aortae in some mutant embryos, or severely malformed vessels with thin walls, a disorganized appearance, and a lack of vascular integrity in other embryos (57, 58). The presence of PECAM-positive cells in mutant embryos led to the conclusion that disruption of *mef2c* didn't interfere with the differentiation of endothelial cells, but rather pointed to a role in organization of endothelial cells into a vascular network (57). The other noteworthy observation from these studies was that *mef2c* is in fact expressed in endothelial cells, a point that had not been demonstrated prior to the mouse knockout studies (57). Previous to this work, it had been appreciated that *mef2c* was expressed in SMCs, although before the work contained in this dissertation, no specific smooth muscle target gene of MEF2C had been identified.

In summary, before the work contained in this dissertation, all that we knew about MEF2C's role in the vasculature was that it was expressed in both endothelial and smooth muscle and that it was necessary for proper vascular development. However, nothing was known about the genes upstream or downstream in the developmental pathway of either endothelial or SMCs. We were interested in all of these questions, so my work focused on understanding the regulation and function of MEF2C in both endothelial cells and vascular smooth muscle cells. In Chapter 2, I explain how we identified the *HRC* gene as the first described MEF2 target in smooth muscle. In Chapter

3, I describe how we used evolutionary conservation to identify seven different tissue-specific modular enhancers in a screen of the *mef2c* locus. Then, in Chapter 4, I describe how we have identified a necessary and sufficient 44 bp endothelial enhancer from the *mef2c* locus that we hope will provide invaluable information about vascular development and transcriptional regulation in general.

Chapter 2

MEF2-Dependent Regulation of *HRC*

Introduction

The *HRC* gene encodes the histidine-rich calcium-binding protein (HRCBP), which is expressed in the sarcoplasmic reticulum (SR) of cardiac and skeletal muscle and within calciosomes in arterial smooth muscle (69-71). HRCBP is found in the lumen of the junctional SR, which is where the ryanodine receptor releases calcium into the cytoplasm (69, 72-74). HRCBP binds calcium in vitro with high capacity and low affinity (69, 75), and while its function is not known, its expression pattern, subcellular localization to the lumen of the SR, association with components of the calcium release channel complex, and calcium binding properties suggest that it may play a role in calcium release during excitation-contraction coupling (69, 70, 72, 73, 76).

MEF2 factors are known to be important early transcriptional regulators of differentiation in skeletal and cardiac muscle cells, but before this work, no transcriptional targets of MEF2 factors in smooth muscle had yet been defined in an *in vivo* context. By contrast, SRF, another member of the MADS family of transcription factors, has been known to regulate the transcription of multiple smooth muscle genes through its consensus binding site: CC(A/T)₆GG, also known as a CarG box (77). In fact, there are only a few examples of genes with known smooth muscle enhancers that do not contain a CarG box. These genes include the *cysteine-rich protein 2 (CRP2)* gene and the *aortic carboxypeptidase-like protein (ACLP)* gene. The enhancer and promoter sequences of these two genes lack both CarG boxes and MEF2 binding sites (78, 79). In this chapter, I will discuss how we identified the *HRC* gene as the first known target of MEF2 in smooth muscle, and furthermore, how we determined that *HRC* appears to be independent of SRF for its transcription in cardiac, skeletal and arterial smooth muscle.

Results and Discussion

Identifying the *HRC* Enhancer

The first step that we took in defining the transcriptional regulation of the *HRC* gene was to identify a DNA fragment from the *HRC* locus that contained promoter and enhancer activity in skeletal, cardiac or arterial smooth muscle. We started by looking at the sequence surrounding the transcriptional start site. A 2726 bp fragment starting at a BamHI site at 2609 bp upstream of the transcriptional start site and ending at a Psp1406I site at 117 bp downstream of the transcriptional start site was tested for enhancer and promoter activity in transfection assays in tissue culture. It was cloned into a *chloramphenicol acetyl transferase* (*CAT*) reporter plasmid such that the transcriptional start site of the *HRC* gene would be used to initiate translation at the start codon in the *CAT* message. We then transfected this *HRC-CAT* reporter plasmid into 10T1/2 fibroblasts, proliferating C2C12 skeletal myoblasts, and differentiating C2C12 skeletal myotubes to determine whether this 2726 bp of sequence was sufficient to direct *CAT* expression in cultured myoblasts (Fig. 1). As positive and negative controls we used the *myogenin* promoter, which is known to direct expression only in skeletal muscle (80-82), and a promoterless *CAT* reporter gene construct (Fig. 1). In these experiments, we found that the *HRC* enhancer directed strong expression in myoblasts (Fig. 1, lane 5) and myotubes (Fig. 1, lane 8), but not in fibroblasts (Fig. 1, lane 2). These results were nearly identical to the levels of transcription activated by the *myogenin* promoter in both myoblasts and myotubes (Fig. 1 lanes 6 and 9 respectively).

Thus, we had identified a region of the *HRC* gene that exhibited enhancer activity in cultured skeletal muscle cells, but we still didn't know if this enhancer could function

in vivo or whether it would exhibit tissue specificity in vivo. In order to answer these questions, we tested the 2726 bp *HRC* fragment in a transgenic mouse model. The fragment was cloned into the promoterless *lacZ* reporter plasmid, AUG- β -gal, which was used to make transgenic mice by pronuclear injection (83). Transgenic embryos were then collected and stained for β -galactosidase expression at various stages of development.

At 8.5 dpc, we found that the 2726 bp construct directed *lacZ* expression to the myotomal compartment of the rostral somites and to the myocardium in the developing heart (Fig. 2A). At 9.5 dpc, the expression of *lacZ* became stronger and expression in the somites began to expand a little more caudally, but the pattern remained mostly the same as at 8.5dpc (Fig. 2B). By 11.5 dpc, expression could be seen in arterial smooth muscle and both the hypaxial and epaxial compartments of the somites (Fig.2 C, E, F, and G). Smooth muscle expression was almost completely limited to arterial smooth muscle. Smooth muscle of the trachea, esophagus, and cardinal vein did not express the transgene (Fig.2G), which was consistent with the endogenous *HRC* expression pattern, which includes arterial smooth muscle but excludes smooth muscle from other tissues (71). The only exception to this tissue restriction was some very weak, patchy expression of *lacZ* in the smooth muscle of the vena cava that was occasionally seen (data not shown). At 13.5 dpc, expression was evident in just about every skeletal muscle in the embryo (Fig.2D), and the cardiac expression directed by the *HRC* enhancer was primarily restricted to the ventricles (Fig.2H).

After 13.5 dpc, the expression pattern of *lacZ* directed by the 2726 bp construct remained relatively unchanged throughout the rest of development and in adulthood (data

not shown). In summary, these results demonstrate that the 2726 bp construct is sufficient to direct expression to skeletal, cardiac, and arterial smooth muscle during embryonic development in vivo.

An Evolutionarily Conserved Sequence Functions as a Minimal *HRC* Enhancer

Within the 2726 bp construct is a 141 bp region of mouse/human homology located between 608 and 468 bp upstream of the transcriptional start site. This sequence is more than 80% conserved between mouse and human, and was used to direct our search for the minimal *HRC* enhancer. We first made a construct that spanned the sequence from -770 to +117. This enhancer still directed strong *lacZ* expression to skeletal muscle, but only weak expression to cardiac and arterial smooth muscle in transgenic mice (Fig. 3 construct 2). When this construct was further reduced to include only the sequence from -510 to +117, expression in all three muscle cell types was completely eliminated (Fig. 3 construct 3). Most of the mouse/human homology is contained in the -770 to -510 fragment, so we were interested to know if this small fragment was necessary for *HRC* expression. To test whether this region of the enhancer was required, we made a construct of the sequence from -2609 to +117 with a deletion from -770 to -510. This construct also could not direct any expression of *lacZ* any of the three muscle lineages (Fig. 3 construct 4), indicating that the 261 bp between -770 and -510 are absolutely necessary for *HRC* expression in vivo.

Next, we asked whether this 261 bp fragment was sufficient for enhancer activity in vivo. To address this question, we placed the 261 bp alone into the HSPP68-*lacZ* reporter plasmid so that if the 261 bp contained a functional enhancer, it could act with

the minimal HSP68 promoter to drive expression of the *lacZ* reporter gene. This construct was able to drive strong expression in skeletal muscle and weak expression in cardiac and arterial smooth muscle (Fig. 3, construct 5). Taken together, the results of these deletional analyses demonstrated that a minimal enhancer exists between 770 and 510 bp upstream of the transcriptional start site, and this conserved region is necessary and sufficient to direct expression in vivo to all three muscle cell types. It appears that there are elements in the sequence between —2609 and —770 that assist the necessary minimal enhancer in directing expression to cardiac and smooth muscle, but clearly the most important elements are located between —770 and —510, which includes most of the mouse/human homology found in the original 2726 bp enhancer.

The *HRC* Enhancer Contains a Functional, Evolutionarily Conserved MEF2 Site

We closely examined the —770 to —510 sequence with special attention paid to the sequence that was conserved between mouse and human, and found that a completely conserved, consensus MEF2 site was contained within this critical region (Fig. 4B). To verify that this consensus MEF2 site was indeed a functional MEF2 binding site, we tested its ability to bind to MEF2 in an electrophoretic mobility shift assay (EMSA). We found that the conserved MEF2 site was strongly bound by MEF2A in vitro (Fig. 5A lane 2). This binding ability was specific to the HRC MEF2 site as shown by the ability of an unlabeled HRC MEF2 site to effectively compete for MEF2 binding (Fig. 5A lane 3), and the inability of a 100-fold excess of unlabeled mutated HRC MEF2 site to compete for MEF2 binding (Fig. 5A lane 4). Furthermore, a 100-fold excess of an unlabeled MEF2 site from the *myogenin* promoter (82) also effectively competed for MEF2A binding to

the HRC MEF2 site (Fig. 5A lane 5), while the same concentration of the mutated *myogenin* promoter MEF2 site (82) could not (Fig. 5A lane 6). When the mutated HRC MEF2 site was used as the labeled probe itself, it showed no ability to bind to MEF2A (Fig. 5A lane 6). These results demonstrate that the conserved MEF2 site from the *HRC* promoter is a *bona fide* MEF2 site that can be bound in a specific manner by MEF2 *in vitro*.

We next tested the ability of MEF2 to bind to the HRC MEF2 site and *trans*-activate the enhancer in cell culture. We co-transfected the *HRC-lacZ* reporter plasmid and the expression plasmid for either MEF2A or MEF2C into 10T1/2 fibroblasts, which provide a silent transcriptional background to test the ability of MEF2 factors to *trans*-activate the *HRC* enhancer (Fig. 5B). The 2726 bp *HRC* enhancer was *trans*-activated by both MEF2A and MEF2C (Fig. 5B, lanes 3 and 5). Mutation of the MEF2 site within the context of the 2726 bp completely eliminated any *trans*-activation by either of the MEF2 factors (Fig. 5B, lanes 3 and 5). These results, along with the results from the EMSA (Fig. 5A), show that the MEF2 site in the *HRC* enhancer can bind to MEF2 factors and allow them to *trans*-activate the enhancer, strongly suggesting that *HRC* is a direct target of MEF2 factors through the conserved MEF2 binding site in the enhancer.

The MEF2 Site in the *HRC* Enhancer is Required for Expression in all Three Muscle Cell Types

After testing the binding and *trans*-activation of the conserved MEF2 site by MEF2 factors *in vitro* and in cell culture, we tested the necessity of the site *in vivo* using the transgenic mouse model. The MEF2 site was mutated in the context of the full-length

2726 bp *HRC* enhancer, cloned into a *lacZ* reporter plasmid, and then used to generate transgenic mouse embryos.

Mutation of the *HRC* MEF2 site completely ablated expression in cardiac and smooth muscle and had a dramatic effect on skeletal muscle expression. The wild type transgene directed expression to cardiac muscle throughout development as well as in adult mice (Fig. 6A, B, C, K, and L). Cardiac expression was strong during midgestational development of the mouse (Fig. 6A, B, and C), and by late gestation was only slightly reduced in expression and restricted almost completely to the ventricles (Fig. 6K). This same expression pattern persisted in adulthood (Fig. 6L). However, expression of *lacZ* in transgenic mice with a mutated MEF2 site in the context of the 2726 bp *HRC* enhancer was completely absent from cardiac muscle throughout development and in adult animals (Fig. 6 E, F, G, O, P).

In smooth muscle, the wild type transgene directed expression to arterial smooth muscle beginning at about 11.5 dpc and continuing throughout development and in adulthood (Fig. 6 C, D, K, L). Expression in arterial smooth muscle was somewhat weaker in the adult than in the embryos, however it was still significantly and homogeneously expressed in arterial smooth muscle even in the adult (Fig. 6 L). The transgene with the mutant MEF2 site, however, did not direct expression to any smooth muscle at any timepoint during development or adulthood (Fig. 6 G, H, O, P). These results show that *HRC* is the first defined target of MEF2 transcription factors in smooth muscle and that activation of transcription by MEF2 is absolutely necessary for *HRC* expression in arterial smooth muscle. It should be noted here that although the esophageal muscle does not express the transgene from the wild type or mutant *HRC* promoters

during embryogenesis (Fig. 2G and 6O), it does express the transgene from the wild type enhancer in the adult esophagus (Fig. 6 L). This esophageal expression in the adult is not in smooth muscle, but rather in skeletal muscle. During the last few days of gestation and continuing through the first three weeks after birth, the smooth muscle in the rostral regions of the esophagus is replaced by skeletal muscle (84), explaining the changes in *lacZ* expression that we see from the embryonic esophagus to the adult esophagus.

In skeletal muscle, the wild type transgene was expressed starting at 9.0 dpc in the myotomal compartments of the rostral somites (Fig. 6A). The expression pattern expanded at 11.5 dpc to include the hypaxial and epaxial skeletal myoblasts in the somites and the small patches of skeletal myoblasts that exist at this stage in the limbs (Fig. 6B and C). By 16.5 dpc, *lacZ* expression was found in all of the skeletal muscle throughout the embryo (Fig. 6J). Mutation of the MEF2 site within the *HRC* enhancer severely reduced the levels of *lacZ* expressed in most skeletal muscle. At 9.0 dpc, *lacZ* staining in the somites was visible (Fig. 6E), but somewhat weaker than the staining observed with the wild type enhancer (Fig. 6A). At 11.5 dpc, *lacZ* expression directed by the mutant enhancer in the somites was still clearly visible (Fig. 6F and G), but considerably weaker than expression directed by the wild type enhancer (Fig. 6B and C). Staining in parts of the forelimbs was also reduced in the embryos containing the mutated MEF2 site, with the exception of the dorsal limb myoblasts which showed stronger staining than that seen in embryos with the wild type transgene (Fig. 6F and G). At 13.5 dpc, a striking difference in *lacZ* expression was apparent between embryos with the wild type enhancer and embryos with the mutated enhancer (Fig. 6I and M). While *lacZ* was expressed strongly in virtually all skeletal muscle in embryos with the wild type enhancer

(Fig. 6I), expression was nearly absent in the skeletal muscle of embryos with a mutated enhancer with only a few faint patches of expression visible at this stage (Fig. 6M). After 16.5 dpc, the results were even more dramatic. The wild type enhancer directed expression throughout all skeletal muscle (Fig. 6J), but the MEF2 mutant enhancer was essentially inactive and virtually no staining was seen in any skeletal muscle after this point (Fig. 6N).

Taken together, the results in skeletal muscle indicate that the MEF2 site is indispensable in the maintenance of *HRC* expression in skeletal muscle, but does not appear to be necessary for the initiation of *HRC* expression. This model explains why the early somitic expression of the mutant enhancer is almost identical to that of the wild type enhancer (Fig. 6A and E), and then weakens until it is absent later in development.

Furthermore, the early overexpression of *lacZ* in the dorsal forelimbs of MEF2 mutant 11.5 dpc embryos supports a model for MEF2-independent initiation of expression in skeletal muscle. Indeed, these data suggest a model in which the MEF2 site may play an early repressive role in this tissue. We believe that when the repression is alleviated by mutation of the MEF2 site, the myoblasts of the dorsal forelimb overexpress the *HRC* transgene, thereby explaining the overexpression in the dorsal forelimbs in the MEF2 mutant 11.5 dpc embryos (Fig. 6F and G). This type of model for MEF2-dependent repression through recruitment of histone deacetylases (HDACs) has been suggested previously (85). In this model, an HDAC/MEF2 complex at the enhancer represses activation of transcription by myogenic bHLH transcription factors at nearby E boxes (85, 86). When the signals for muscle differentiation occur, CaMK mediates the dissociation of HDACs from MEF2 factors via phosphorylation of two serines in class II

HDACs that flank a nuclear localization signal (87). The intracellular chaperone protein 14-3-3 binds to the phosphorylated HDAC, causing it to dissociate from MEF2 and allowing the 14-3-3/HDAC complex to be shuttled out of the nucleus (88-90). This leaves MEF2 free to switch from a repressor to an activator through cooperative interactions with myogenic bHLH factors.

While MEF2 does not appear to be important in the initial activation of *HRC* in skeletal muscle, and may in fact be suppressing it, the complete absence of *lacZ* expression in cardiac and arterial smooth muscle in transgenic mice with a mutated MEF2 site in the *HRC* promoter suggests that MEF2 may be playing a role in the initial activation as well as the maintenance of expression of the *HRC* gene in these tissues. However, even though MEF2 appears to play a critical role in the expression of *HRC* in all three muscle cell types, we do not think that it is the only transcriptional regulator in any of these cell types. Instead, we believe that MEF2 is acting cooperatively with other lineage or tissue-specific transcription factors. It has been well documented that MEF2 factors act cooperatively in skeletal and cardiac muscle with other transcription factors (61, 62, 91), and although no co-regulators of MEF2 have yet been identified in smooth muscle (mainly because no targets of MEF2 had been identified in smooth muscle prior to this work), another MADS domain transcription factor, SRF, has been shown to act in a cooperative manner in smooth muscle (92). We therefore believe that different MEF2 transcriptional co-regulators are playing roles in the transcriptional regulation of *HRC* in each of the three muscle cell types and we are interested to find out what these co-regulators are, particularly in cardiac and smooth muscle.

The *HRC* Enhancer is not Responsive to SRF

We have shown that a 2726 bp fragment of DNA from the *HRC* enhancer can direct expression to cardiac, skeletal, and arterial smooth muscle. We have also shown that a conserved MEF2 site within a critical 261 bp of this enhancer can mediate *trans*-activation of this enhancer by both MEF2A and MEF2C in 10T1/2 fibroblasts in tissue culture and that this MEF2 site is required *in vivo*. The fact that this enhancer directs expression to arterial smooth muscle in what appears to be a MEF2-dependent fashion was exciting to us because a MEF2 target in smooth muscle had not yet been discovered. By contrast, SRF is a well-known regulator of genes in smooth muscle. Moreover, the vast majority of smooth muscle genes for which regulatory elements are known, are regulated at least in part by SRF (77). Therefore, we wanted to determine whether the *HRC* enhancer could also be regulated by SRF. We first searched the entire 2726 bp enhancer for consensus CArG boxes, which are the binding sites for SRF. Although no CArG boxes were found, we could not rule out the possibility that SRF was binding to a non-consensus site or even the MEF2 site itself. We therefore tested the ability of SRF to bind to the MEF2 site *in vitro* and activate the *HRC* enhancer in tissue culture. While MEF2A was able to bind the MEF2 site in an EMSA (Fig. 5C, lane 2), SRF was not (Fig. 5C, lane 5). In the same experiment, SRF was able to very strongly bind to a consensus CArG box from the *smooth muscle alpha-actin (SMaa)* gene (Fig. 5C, lane 9), showing the specificity of SRF binding. Similarly, SRF could not *trans*-activate the *HRC* enhancer in 10T1/2 fibroblasts (Fig. 5D, lane 3) under conditions where MEF2C could *trans*-activate the *HRC* enhancer (Fig. 5D, lane 2) and SRF could *trans*-activate the SMaa enhancer (Fig. 5D, lane 5). These results show that the *HRC* enhancer is not responsive to

SRF. This observation, taken together with the results that identified *HRC* as a MEF2 target in vivo, show that *HRC* is the first example of a MEF2-dependent, SRF-independent smooth muscle gene.

Figure 1

The HRC upstream region contains promoter and enhancer sequences sufficient to direct muscle-specific expression. HRC-CAT (lanes 2, 5, and 8), myogenin-CAT (lanes 3, 6, and 9), and the promoterless CAT-Basic (lanes 1, 4, and 7) reporter plasmids were transfected into fibroblasts (lanes 1 to 3), myoblasts (lanes 4 to 6), or myotubes (lanes 7 to 9). The HRC and myogenin reporter plasmids exhibited no significant activity over background in nonmuscle fibroblasts (lanes 2 and 3), but both reporters were robustly active in myoblasts (lanes 5 and 6) and myotubes (lanes 8 and 9). Data are expressed as a percentage of the activity obtained using a constitutively active SV40-CAT plasmid in each cell type. The data shown represent the mean values obtained in five independent transfections and analyses. Error bars represent the standard errors of the means.

•

Figure 1

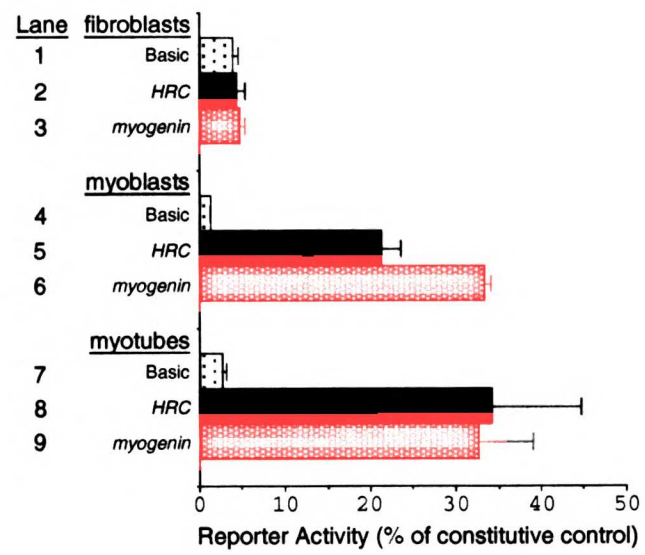


Figure 2

The HRC enhancer directs cardiac, skeletal, and arterial smooth muscle expression in transgenic mouse embryos. A 2,726 bp fragment of the human HRC gene was fused to a lacZ reporter plasmid and used to generate transgenic mice. This fragment of the HRC gene was sufficient to direct expression to all three muscle lineages in the mouse embryo in the pattern of endogenous HRC. (A to D) Representative X-Gal-stained transgenic embryos are shown at 8.5 dpc (A), 9.5 dpc (B), 11.5 dpc (C), and 13.5 dpc (D). The embryos in panels C and D have been cleared in a 1:1 mixture of benzyl alcohol and benzyl benzoate to help visualization of internal structures. Expression was evident at 8.5 dpc in the heart (hrt) and in the myotomal compartment of the somites (S) and by 11.5 dpc in arterial smooth muscle. No expression was observed in venous smooth muscle or in other smooth muscle cell types. (E to G) Transverse sections from X-Gal-stained transgenic embryos at 11.5 dpc. Expression was evident in somites, heart, and arterial vascular smooth muscle, including the dorsal aorta (DA) and branchial arch arteries (BAA). By contrast, expression was not observed in venous smooth muscle, including the cardinal veins (CV). No expression was observed in the smooth muscle of the trachea (Tr) or esophagus (Es) (G). Expression in the heart was restricted to the ventricles (E and F). Bar, 100 μ m. (H) The heart and associated vasculature removed from an HRC-lacZ transgenic embryo at 13.5 dpc and stained with X-Gal. Expression in the heart at 13.5 dpc was restricted to the ventricles. Expression was also evident in arterial vascular smooth muscle, including the aorta (Ao) and subclavian (SubCL) and carotid arteries (Ctd). LA, left atrium; LV, left ventricle; NT, neural tube; RA, right

atrium; RV, right ventricle. Seven independent transgenic lines all displayed nearly identical patterns of expression.

Figure 2

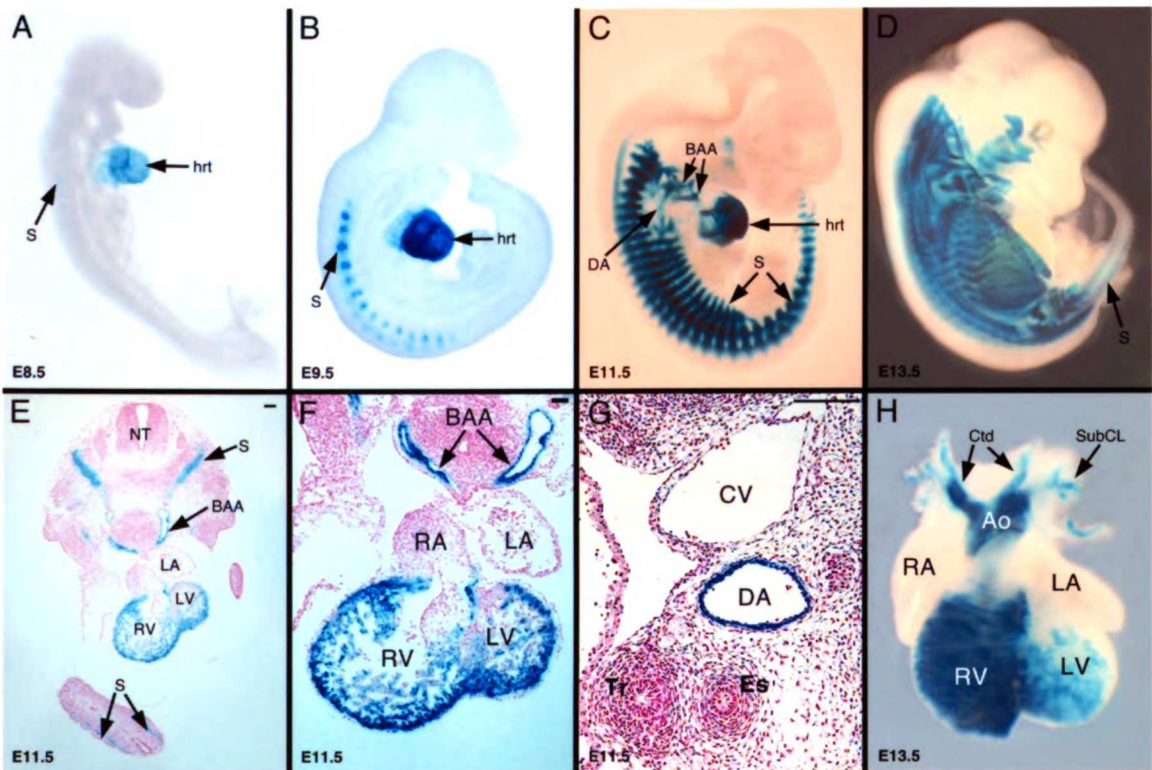


Figure 3

Deletional analysis of the *HRC* upstream region identified a conserved region required for expression *in vivo*. Schematic representations of the various deletion constructs of the *HRC* upstream region analyzed in these studies are shown in the center. Red arrow, *HRC* transcriptional start site; green arrow, transcriptional start site directed by the heterologous HSP68 promoter; blue arrow, *lacZ* translational start site; B, BamHI; N, NcoI; Bg, BglII; P, Psp1406I. Construct number and nucleotides, relative to the *HRC* transcriptional start site at +1, are indicated on the left. Expression of *lacZ* in somites, limbs, heart, and arteries is noted in the columns to the right. +++, very robust, easily detectable expression; +, very weak expression; —, a complete lack of detectable expression. The column on the far right indicates the number of independent transgenic lines or F0 transgenic embryos that expressed *lacZ* in the indicated pattern as a fraction of the total number of transgene-positive F0 embryos or lines examined. For HSP68/510-770 (construct 5), three of the five lines examined expressed *lacZ* in the indicated pattern. The other two F0 transgenic embryos showed no expression of *lacZ*.

Figure 3

Construct		lacZ Expression				#expressing/ #transgenic
		Somite	Limb	Heart	Artery	
1. (-)2609		+++	+++	+++	+++	7/7
2. (-)770		+++	+++	+	+	8/8
3. (-)510		-	-	-	-	0/5
4. Δ510-770		-	-	-	-	0/4
5. HSP68/510-770		+++	+++	+	+	3/5

Figure 4

An evolutionarily conserved noncoding sequence resides in the upstream region of the HRC gene. (A) Schematic representation of the human HRC upstream region. The HRC upstream region (—2609 to +117) was cloned as a BamHI-Psp1406I fragment into CAT and β -galactosidase reporter plasmids such that transcription would start from the HRC transcriptional start site (red arrow) and translation would initiate in the reporter cDNA. Green box, evolutionarily conserved region; black arrow, HRC translational start site; B, BamHI; N, NcoI; Bg, BglII; P, Psp1406I. (B) Sequence alignment of the evolutionarily conserved element from the HRC upstream region from —608 to —468, relative to the transcriptional start site, in the human sequence. The box denotes the evolutionarily conserved MEF2 site.

Figure 4

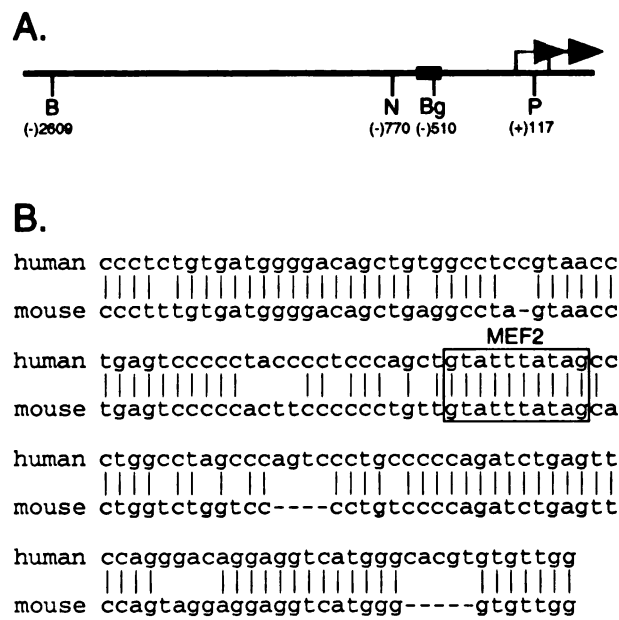


Figure 5

The conserved region of the *HRC* enhancer contains a high-affinity, functional MEF2 site. (A) MEF2 binds specifically to the HRC MEF2 site in vitro. MEF2A was transcribed and translated in vitro and used in EMSA analyses with radiolabeled double-stranded oligonucleotides representing the HRC MEF2 site (lanes 1 to 6) or a mutant version of the HRC MEF2 site (lanes 7 and 8). MEF2 efficiently bound to the HRC MEF2 site (lane 2) but failed to bind to the mutant MEF2 site (lane 8). Binding of MEF2 to the HRC MEF2 site was specific, since a 100-fold excess of unlabeled HRC MEF2 site efficiently competed for binding (lane 3), but a mutant version of the HRC MEF2 site (mHRC) failed to compete for binding even at a 100-fold excess (lane 4). Likewise, an unlabeled control MEF2 site from the *myogenin* gene (My) efficiently competed for binding (lane 5), but a 100-fold excess of a mutant *myogenin* MEF2 site (mMy) did not compete for binding (lane 6). In samples where in vitro-translated proteins were absent (lanes 1 and 7), an equal amount of unprogrammed reticulocyte lysate was included. Lysate-derived, nonspecific mobility shifts are noted. (B) The *HRC* enhancer is activated directly by MEF2 factors through the MEF2 site in the enhancer. MEF2A expression plasmid (lanes 3 and 4), MEF2C expression plasmid (lanes 5 and 6), or parental expression vector (lanes 1 and 2) was cotransfected with a full-length *HRC-lacZ* reporter plasmid (lanes 1, 3, and 5) or a mutant version of that reporter containing a disrupted MEF2 site (lanes 2, 4, and 6) into 10T1/2 fibroblasts. The parental expression vector failed to significantly activate the *HRC* enhancer (lane 1). MEF2A and MEF2C were each able to significantly *trans*-activate the *HRC*-dependent reporter (lanes 3 and 5, respectively). Neither MEF2A nor MEF2C activated the MEF2 mutant enhancer (lanes 4

and 6, respectively). The data shown represent the mean values obtained in three independent transfections and analyses. Error bars represent the standard errors of the means. (C) The *HRC* MEF2 site is not bound by SRF. Either MEF2A (lanes 2 to 4) or SRF (lanes 5 to 7 and 9 to 11) was transcribed and translated in vitro and used in EMSA analyses with radiolabeled double-stranded oligonucleotides representing the *HRC* MEF2 site (lanes 1 to 7) or the SMaa intronic CArG box (lanes 8 to 11). MEF2 efficiently bound to the *HRC* MEF2 site (lane 2), whereas SRF was completely unable to bind to the *HRC* MEF2 site (lane 5) under conditions in which it efficiently bound to the SMaa CArG box (lane 9). In samples where in vitro-translated proteins were absent (lanes 1 and 8), an equal amount of unprogrammed reticulocyte lysate was included. Lysate-derived, nonspecific mobility shifts are noted. Wild-type (*HRC* and CArG) and mutant (m*HRC* and mCArG) competitors were used at a 100-fold excess where indicated. (D) The *HRC* enhancer is not *trans*-activated by SRF. Expression plasmids for MEF2C (lane 2), SRF (lanes 3 and 5), or the parental expression vector (lanes 1 and 4) were cotransfected with a full-length *HRC-lacZ* reporter plasmid (lanes 1 to 3) or a SMaa-*lacZ* reporter plasmid (lanes 4 and 5) into 10T1/2 fibroblasts. SRF failed to activate the *HRC* reporter (lane 3) under conditions in which MEF2C activated the *HRC* reporter more than 10-fold (lane 2) over the background level of activation indicated by parental expression vector cotransfection (lane 1). By contrast, SRF activated the SMaa reporter in the same experiment more than 16-fold (lane 5) over the background level of activation indicated by parental expression vector cotransfection (lane 4). The data shown represent the mean values obtained in three independent transfections and analyses. Error bars represent the standard errors of the means.

Figure 5

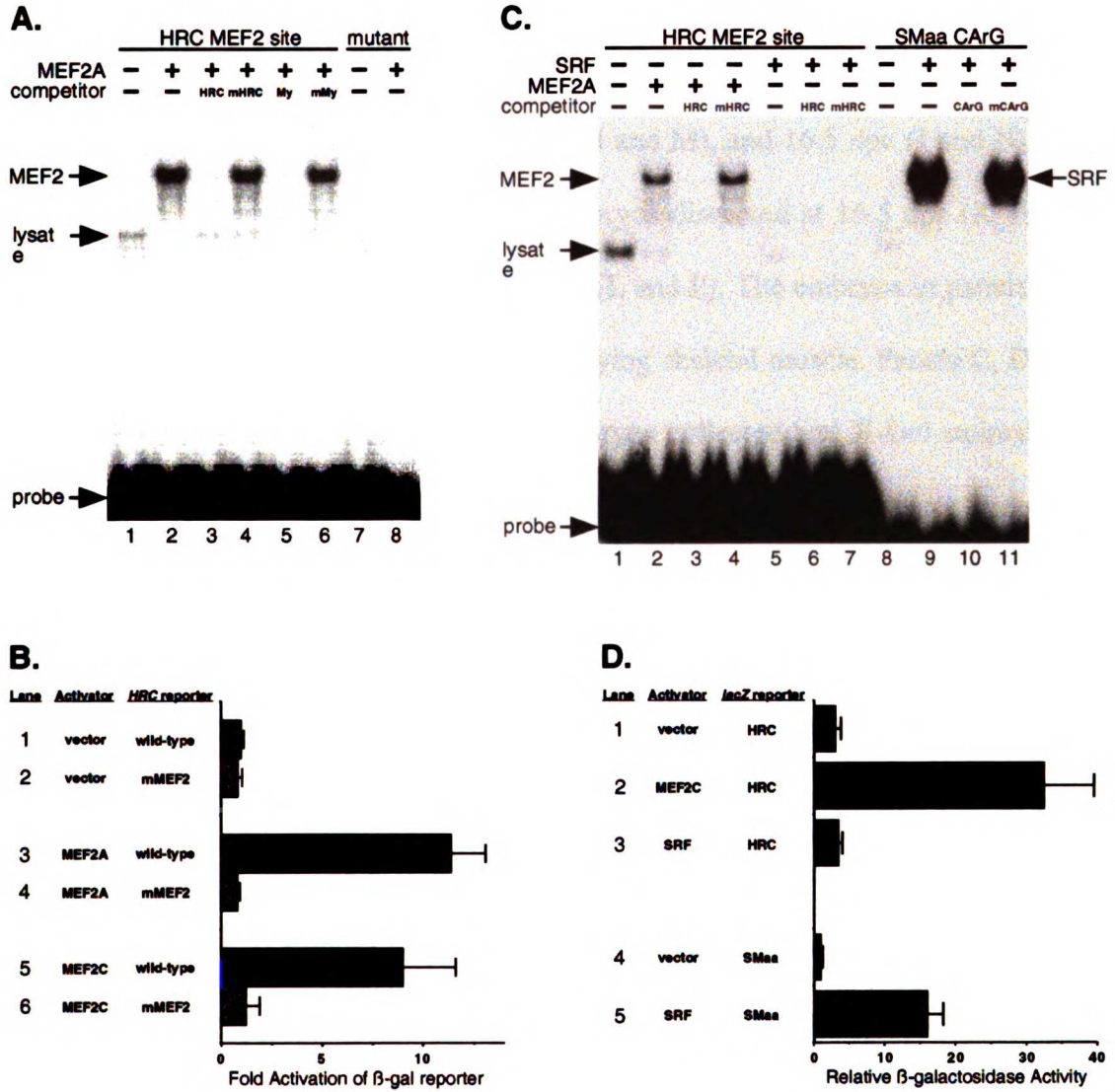
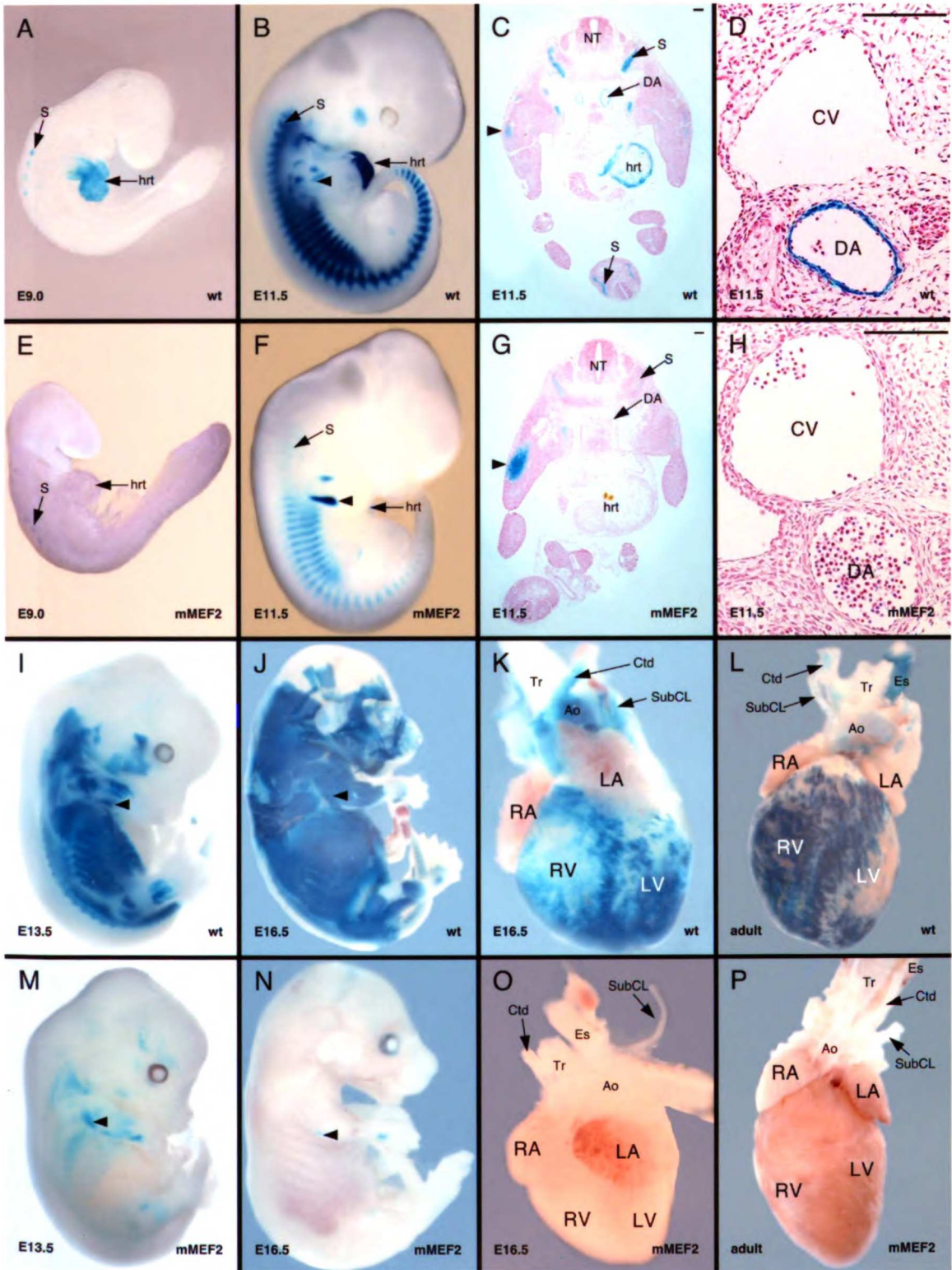


Figure 6

The MEF2 site in the HRC enhancer is required for expression in cardiac, skeletal, and arterial smooth muscle *in vivo*. Wild-type MEF2 site (A to D and I to L) and mutant MEF2 site (E to H and M to P) HRC-lacZ transgenic mice were analyzed for expression *in vivo*. Representative X-Gal-stained, transgenic embryos are shown at 9.0 dpc (A and E), 11.5 dpc (B and F), 13.5 dpc (I and M), and 16.5 dpc (J and N). X-Gal-stained hearts are shown from transgenic embryos dissected at 16.5 dpc (K and O) or transgenic adults dissected at 16 weeks of age (L and P). The embryos in panels J and N have been skinned to help visualize the underlying skeletal muscle. Panels C, D, G, and H show transverse sections of transgenic embryos collected and X-Gal stained at 11.5 dpc. Bar, 100 μ m. The 2,726-bp wild-type (wt) HRC enhancer construct directed lacZ expression to the heart throughout embryonic development (A and B). By 11.5 dpc, expression was restricted to the ventricles (C), and the ventricle-restricted cardiac expression continued in the fetal (K) and adult (L) heart. The mutant MEF2 2,726-bp HRC enhancer construct (mMEF2) failed to direct expression to the heart at any stage in the embryo (E to G), fetus (O), or adult (P). The wild-type construct directed strong expression to arterial smooth muscle, including the dorsal aorta, beginning at 11.5 dpc (D). Arterial smooth muscle expression was also evident in the fetus (K) and adult (L). Smooth muscle expression was restricted to arteries. Note that the esophagus staining in the adult (L) represents skeletal muscle in the adult esophagus. The MEF2 mutant enhancer failed to drive lacZ expression in smooth muscle at all stages, including 11.5 dpc (G and H), 16.5 dpc (O), and adult (P). The wild-type transgene was robustly expressed in skeletal muscle in both the hypaxial and epaxial domains at 11.5 dpc (B and

C). The MEF2 mutant transgene was also expressed in both hypaxial and epaxial myotomes, but the level of expression was much weaker at 11.5 dpc (F and G). Both the wild-type (B and C) and mutant MEF2 (F and G) enhancers directed expression to the dorsal limb muscles at 11.5 dpc. The wild-type enhancer drove strong lacZ expression in all skeletal muscles at 13.5 dpc (I) and 16.5 dpc (J). The mutant MEF2 enhancer directed only very weak skeletal muscle expression at 13.5 dpc (M), and expression was essentially absent by 16.5 dpc (N). Ao, aorta; Ctd, carotid artery; CV, cardinal vein; DA, dorsal aorta; Es, esophagus; hrt, heart; LA, left atrium; LV, left ventricle; NT, neural tube; S, somite (myotome); RA, right atrium; RV, right ventricle; SubCL, subclavian artery; Tr, trachea. Arrowheads denote expression in dorsal limb muscles.

Figure 6



Chapter 3

Evolutionary Conservation of Regulatory

Elements of *Mef2c*

Introduction

Because *mef2c* plays a crucial role in muscle development, understanding its regulation is key to a better understanding of the molecular pathways controlling cardiogenesis, vasculogenesis, and myogenesis, not to mention the possible insights that we might gather on other processes such as neurogenesis and hematopoiesis. With this goal in mind, we began searching for tissue-specific enhancers of *mef2c* with four assumptions: 1) that *mef2c* would have several modular, tissue-specific enhancers; 2) that these enhancers would be present in the 5' upstream region of the gene or contained within one of the introns; 3) that the enhancers would be able to direct expression of a *lacZ* reporter gene fused to an HSP68 promoter; 4) and that each enhancer would be contained within a short module that would be no larger than a few hundred base pairs.

As an initial analysis to identify *mef2c* regulatory elements, a BAC transgenic mouse line was generated to determine if enhancer elements were present in a large region of the *mef2c* gene. Briefly, a *lacZ* reporter gene was inserted into the BAC clone, GS133, which spans 120 Kb of the *mef2c* gene and upstream sequence. The *lacZ* reporter gene was inserted into the exon encoding the highly conserved MADS domain. This recombinant was used to make transgenic mouse lines that incorporated the reporter BAC into their genomes, and expressed the *lacZ* reporter in the complete *mef2c* expression pattern (Fig. 7) (93). This result indicated that regulatory elements sufficient to direct *mef2c* expression were contained within the 120 Kb encompassed by the GS133 BAC.

To identify specific enhancer elements within the *mef2c* locus, we compared the sequence of the mouse *mef2c* gene to the sequences of the human and chick *mef2c* genes in order to identify areas of high conservation in noncoding regions. These sequence

comparisons identified several regions of conservation, which were each tested independently for enhancer activity in transgenic mice. This was performed by cloning each of the conserved elements into the transgenic reporter plasmid HSP68-*lacZ* (94) followed by oocyte microinjection. Using this method to screen the *mef2c* locus, we were able to identify seven separate modular enhancers that were sufficient to direct tissue-specific expression of a *lacZ* transgene in vivo.

Results and Discussion

Sequence Comparison and Selection of Candidate Fragments

We compared the mouse *mef2c* sequence from the GS133 BAC with the human *mef2c* sequence and found 39,795 bp of homology out of 120,401 bp total in the BAC. However, because this homology was broken up into small pieces and spread throughout the BAC, the mouse/human homology did not significantly narrow our search area (Fig. 8). Humans and mice shared a common ancestor approximately 60 million years ago, however chickens and mice shared a common ancestor 310 million years ago, giving those two genomes an extra 250 million years to diverge. When we compared the mouse and chicken sequences, we found that only 4,714 bp or 3.9% of the noncoding sequence showed significant homology. In addition to drastically reducing the percentage of conserved sequence, the mouse/chick homology clustered into distinct pockets (Fig. 8). Based on both the mouse/human and mouse/chick homology, we chose ten fragments of sequence to test for enhancer activity in transgenic mice.

Screening Fragments for Enhancer Activity

The ten fragments chosen to test for enhancer activity were cloned into the transgenic reporter plasmid HSP68-*lacZ* and used to generate *lacZ* transgenic mice. From the ten fragments tested in this manner we discovered seven different enhancer elements: three neural crest enhancers, two endothelial enhancers, a skeletal muscle enhancer and an anterior heart field enhancer. Every fragment that was shown to exhibit enhancer activity in our original screen contained at least one region of mouse/chick homology. Conversely, the two fragments that did not contain any mouse/chick homology (F2 and

F3) lacked enhancer activity. In addition, two fragments that did contain regions of mouse/chick homology (F4 and F5), also lacked detectable enhancer activity under the conditions in which we screened embryos for β -gal activity.

Using Evolutionary Conservation to Delineate Minimal Enhancers

Since all of the fragments that exhibited enhancer activity also contained small regions of mouse/chick homology, we used this homology to direct our search for the minimal enhancer elements. F1, the first neural crest enhancer, contained several pockets of mouse/chick homology which were used to quickly delineate the minimal enhancer to 3 Kb of sequence, and soon thereafter, 1.3 Kb. In this case the mouse/chick homology remained instructive for determining the minimal enhancer, and eventually, for finding the *cis*-acting elements of the enhancer, which were found within one of the regions of mouse/chick homology.

F6, the anterior heart field enhancer, also contained several pockets of mouse/chick homology. This time, however, the mouse/chick homology was not useful in determining the minimal enhancer, which was mapped to an area that was still conserved between mouse and human but not between mouse and chick (93). 73K, the skeletal muscle enhancer, contained a large region of mouse/chick homology in which several necessary transcription factor binding sites were found (95). F7, the first endothelial enhancer, has three pockets of mouse/chick homology. Like F1, the minimal enhancer for F7 corresponded to one of these pockets of homology (96). F10, the fragment that possessed both endothelial and neural crest enhancer activity, had only two pockets of mouse/chick homology. However, when we mapped the minimal enhancers, we found that the endothelial enhancer was located in one pocket of mouse/chick homology, while

the neural crest enhancer mapped to a region that contained the other pocket of mouse/chick homology. F9, the third neural crest enhancer, contains several pockets of mouse/chick homology, but has not been investigated enough at this point to determine whether this homology will aid in determining the minimal enhancer elements.

Of the minimal enhancers located so far, four out of five were found to contain significant mouse/chick homology. In fact, using the mouse/chick homology has been the most frequently used method for determining where we look for the minimal enhancers, and in most cases, this information has been very helpful in predicting where these minimal enhancers are. This likely reflects the notion that the core enhancer elements are ancient and have been conserved over evolutionary time.

Using Evolutionary Conservation to Find Necessary Regulatory Elements

We have also been able to use the mouse/chick homology to locate the necessary transcription factor binding sites within the minimal enhancers. In four out of the five enhancers that we have found necessary binding sites for, these sites were located in regions of mouse/chick homology. The one enhancer where necessary sites have been found outside of the mouse/chick homology is the anterior heart field enhancer, F6, which did not contain any mouse/chick homology within its minimal enhancer.

In addition to comparing the mouse *mef2c* sequence with its human and chicken counterparts, we also compared the mouse and pufferfish *mef2c* sequences. From this comparison, we found that there were only 569 bp of homology from the 120,401 bp in the BAC. Less than 0.5% of the sequence was homologous, and more than half of the sequence that was homologous, was exonic sequence. However, F1, F7, and F10 each

contained a small pocket of mouse/pufferfish homology. In both F1 and F7, the mouse/pufferfish homology did not map to the minimal enhancer elements, but in F10 it did map to the endothelial enhancer. Remarkably, when we made a construct that included only the small pocket of mouse/pufferfish homology from F10, the sequence was sufficient to direct expression to the entire endothelium (Fig. 11I).

Analysis

As for the optimal amount of homology or divergence to be used in a search for regulatory elements, the current studies described here show that different levels of homology are useful for different aspects of an enhancer search. Having a wide array of sequences from which differing levels of homology can be obtained is ideal because one level of homology may be useful for determining which regions to screen while another level of homology may be more useful for finding the necessary or sufficient enhancer elements.

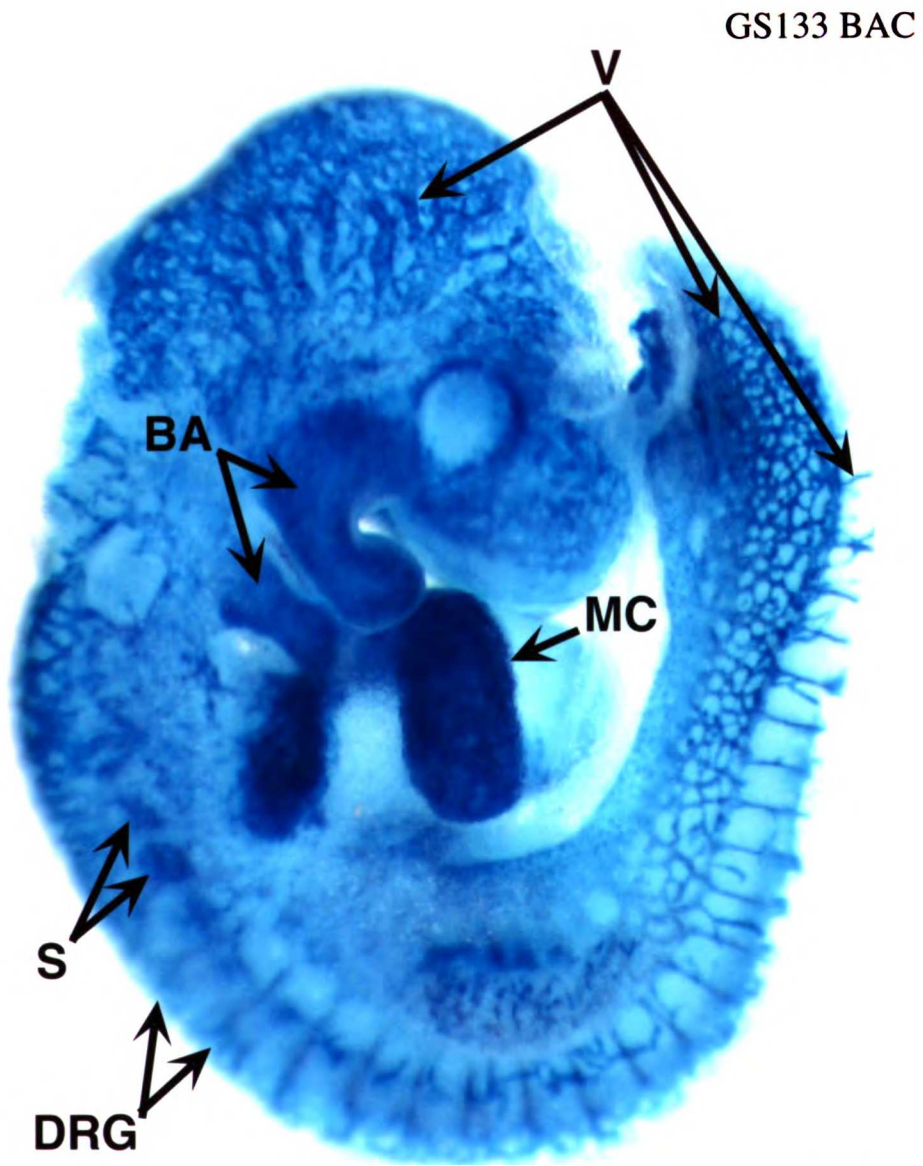
For the *mef2c* gene, we found that there was too much homology between the human and mouse sequences to efficiently screen the whole locus. However, when we used the mouse/chick homology to identify core pockets of homology and then extended these pockets outward using the mouse/human homology, we became quite efficient at screening for enhancer elements. The mouse/chick homology also proved to be very useful for defining minimal enhancers and locating necessary transcription factor binding sites, however, in the case of the anterior heart field enhancer, it failed to predict the minimal enhancer and the mouse/human homology was used instead.

We discovered in our studies that great variations in levels of homology could be instructive in different aspects of defining enhancer elements. This was probably best illustrated in the discovery of the neural crest and endothelial enhancer elements in F10. The fragment was chosen based on its mouse/chick and mouse/human homology. The two minimal enhancers were then separated and defined based on the mouse/chick homology. A small, 44 bp enhancer was then defined for the endothelial expression based solely on 44 base pairs of mouse/pufferfish homology. This example shows how different levels of homology can be useful at different stages of an enhancer search whether 33% of the sequence contains significant homology, or only 0.5% of the sequence contains significant homology.

Figure 7

The 120 Kb GS133 *lacZ* transgenic BAC directs expression to all tissues that express *mef2c* at 9.5 dpc including the myocardium (MC) of the heart, the branchial arches (BA), the dorsal root ganglia (DRG), the myotomal compartment of the somites (S), and the vasculature (V).

Figure 7

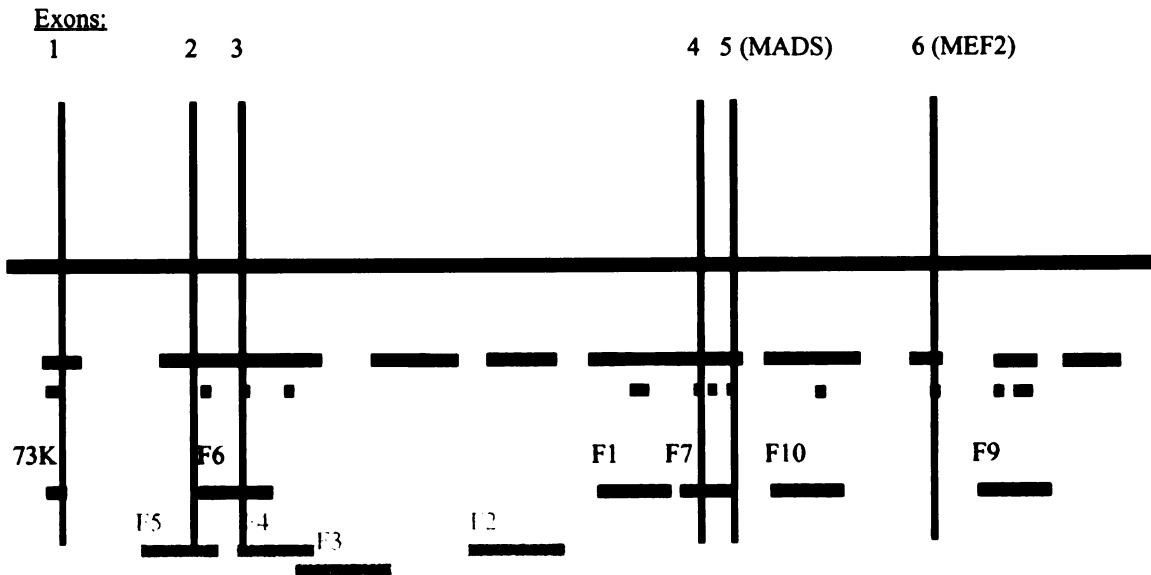


E 9.5

Figure 8

Mouse, human, and chick homology in the GS 133 BAC (120,401 bp), which includes the first six exons of the *mef2c* gene. Mouse/human homology is represented by the blue lines, and mouse/chick homology is represented by the red lines. Fragments that contained enhancer activity are represented by the green lines. Fragments that contained no detectable enhancer activity are represented by the gray lines. The vertical black lines represent *mef2c* exons.

Figure 8



Chapter 4

A 44 bp *Mef2c* Enhancer is Sufficient to

Direct Expression to Vascular Endothelium

Introduction

Endothelial cells are one of the cell types that express MEF2C, but for which very little is known about MEF2C's role in development. What we do know is that when the *mef2c* gene is inactivated in mice, *mef2c* null embryos die by 10.0 dpc (57), approximately the same gestational age as the *flt-1*, *flk-1*, and *Tie-2* deficient embryos die (4, 5, 31). In addition, *mef2c* null embryos have severe vascular defects: the yolk sac vasculature is absent and major blood vessels such as the cardinal veins and dorsal aortae often fail to form (57). In the instances where these major vessels do form, they are abnormally thin-walled and lack integrity (57).

The ETS family of transcription factors has been shown to play an important role in the transcription of several vascular-specific genes. ETS family members are transcription factors which contain the conserved ETS DNA binding domain, which folds into a winged helix-turn-helix motif and binds to the consensus ETS-binding sequence, **RSMGGAWRH**, in the promoter and enhancer sequences of its target genes (97-100). Within the ETS-binding site, the core GGA sequence indicated in bold type is considered to be indispensable for ETS factor binding. The variable flanking sequences of the 4 base pairs that surround the core GGA sequence on either side appear to play a role in specificity of binding within the ETS family, but these specificities have not yet been clearly defined (100-103). The *flk-1*, *flt-1*, *tie*, and *tie-2* genes all depend on at least one **ETS** site in their promoter or enhancer for their transcriptional regulation (53-56).

In order to elucidate the upstream pathways leading to *mef2c* transcription and subsequent cell differentiation, we undertook a screen of the *mef2c* gene for cis-acting elements that control *mef2c* expression in different tissues as described in Chapter 2. One

of the elements that we identified from this screen was a 5.6 KB fragment (F10), which drove *lacZ* expression in the vasculature, branchial arches, and craniofacial mesenchyme at 9.5 dpc. This staining pattern was consistent with transgene expression in endothelial cells and neural crest derivatives. We have subsequently located the neural crest and vascular endothelial elements to two separable pieces of the original 5.6 Kb. The neural crest element has been located to a 1.2 Kb subfragment, and the endothelial element has recently been located to a mere 44 base pairs which are both necessary and sufficient to direct expression of the *lacZ* reporter to the vascular endothelium. Within this 44 bp we have found two Ets factor binding sites and an E-Box which are necessary for endothelial expression, and we continue to look for other transcription factor binding sites.

Results and Discussion

Identification of Closely Linked Endothelial and Neural Crest-Specific Enhancers

From the screen described in Chapter 2, several tissue-specific modular enhancers were located throughout the noncoding upstream and intronic sequences of the *mef2c* gene. The F10 fragment was an approximately 5.6 Kb region located within intron 5, starting at bp 77,569 and ending at bp 83,118 of the GS133 BAC. This 5,550 bp fragment, when cloned into an HSP68-*lacZ* reporter plasmid and subsequently used to create transgenic mice, directed expression of the *lacZ* reporter gene to the vascular endothelium, branchial arches, and craniofacial mesenchyme of 9.5 dpc transgenic embryos (Fig. 9F).

The expression pattern of this 5.6Kb-HSP68-*lacZ* construct was further examined in stable mouse lines. At 7.5 dpc we began to see staining in the embryo's head and some faint spots in the yolk sac (Fig. 9A). By 8.0 dpc, the head staining became stronger and some staining in the future dorsal aortae was visible (Fig. 9B and C). We also observed staining of the vascular plexus as it began to form in the yolk sac at 8.0 dpc (Fig. 9B). At 8.5 dpc, staining in the head was readily apparent (Fig. 9D), the dorsal aortae expressed the transgene along their entire length, and we saw staining in the endocardium of the recently formed heart (Fig. 9D). By 9.0 dpc, the vascular plexus was formed and displayed transgene expression throughout the endothelium (Fig. 9E). At 9.5 dpc we saw the clearly endothelial pattern emerge as blood vessels throughout the embryo expressed the transgene (Fig. 9F). In addition, staining in the endocardium, branchial arches and craniofacial mesenchyme of the 9.5 dpc embryo was apparent (Fig. 9F), consistent with

the neural crest expression pattern at this stage. In cross-section, it was clear that the **vascular** and cardiac staining was due to expression in the inner endothelial lining of the **blood** vessels and heart (Fig. 9G). At 11.5 dpc, endothelial staining remained strong **throughout** the entire endothelium, masking some of the neural crest staining that became **more** narrowly expressed in the dorsal root ganglia (DRG), melanocytes, and parts of the **mandible**, branchial arches and trunk of the embryo (Fig. 9H). Endothelial staining **remained** strong at 13.5 dpc and later throughout the rest of development and in **adulthood** (Fig. 9I).

In summary, endothelium was ubiquitously stained throughout the embryo at **every** stage of development starting with the first few patches of differentiating **endothelial** cells in the blood islands in the yolk sac at 7.5 dpc and the newly formed **dorsal aortae** in the embryo at 8.0 dpc. Staining remained strong throughout development **in** endothelial cells lining arteries, veins, capillaries and the heart, lasting well into **adulthood**. Strong staining was also seen early in development starting at 7.5 dpc in an **expression** pattern reminiscent of the neural crest.

Deletions Within the 5.6 Kb F10 Fragment Separate the Endothelial and Neural Crest Enhancers

We wanted to define minimal enhancers within the 5.6 Kb F10 fragment that **would** be sufficient to direct expression to either endothelium or neural crest. We **reasoned** that these two expression patterns might be separable into two distinct enhancer **elements** because the cell types come from different lineages and many of the regulatory **factors** present in endothelial cells are absent in neural crest cells. We based our

deletional analysis on the evolutionary conservation between the mouse, chicken, and pufferfish sequences (Fig. 10A). When these sequences were compared, we found that the 5.6 Kb F10 fragment contained two pockets of homology that were conserved between mice, humans, and chickens. The first was a 220 bp sequence that was 82% conserved starting at bp 81,075 and ending at bp 81,294 of the GS133 BAC, and the second was a 159 bp sequence that was 72% conserved starting at bp 82,256 and ending at bp 82,414 of the GS133 BAC. We also found a small 44 bp sequence within the 220 bp of mouse/chick homology that was 88% conserved between mouse and pufferfish starting at bp 81,169 and ending at bp 81,212 of the GS 133 BAC. Since all of the mouse/chick and mouse/pufferfish homology was contained in the last 2.1 Kb of the 5.6 Kb fragment, the first subfragment that we tested for enhancer activity in transgenic mice was the 2,104 bp from 81,015 to 83,118, which contained all of the conserved sequences.

We cloned the 2.1 Kb fragment into the HSP68-*lacZ* reporter plasmid (Fig. 10B), and used this construct to create transgenic mice, which were analyzed at 9.5 dpc in the **F₀** generation. From this construct we only managed to generate one transgenic embryo, which showed strong staining in the craniofacial mesenchyme, branchial arches and endothelium (Fig. 11C). From this result, we concluded that the neural crest and endothelial regulatory elements were contained within this 2.1 Kb.

Next, we split the 2.1 Kb fragment into two subfragments that were roughly 900 bp and 1.2 Kb in size. The 889 bp fragment starts at 81,015 and ends at 81,903, and includes 220 bp of mouse/chick homology and 44 bp of mouse/pufferfish homology (Fig. 10B). The 1.2 Kb fragment starts at 81,898 and ends at 83,118 and includes 159 bp of mouse/chick homology (Fig. 10B). These two subfragments were each independently

cloned into the HSP68-*lacZ* reporter plasmid and used to generate transgenic mice. We found that the 1.2 Kb fragment (F10NC) directed expression of *lacZ* to the branchial arches, craniofacial mesenchyme, and DRGs of 9.5 dpc F₀ transgenic embryos (Fig 11E), consistent with neural crest derivatives (104-106). Stable lines of mice containing the F10NC construct were created and analyzed at 11.5 dpc as well. The 11.5 dpc transgenic embryos express the transgene in melanocytes visible in the head, DRGs, and in specific regions of the branchial arches, mandible and trunk of the embryo, again consistent with an expression pattern consisting of neural crest derivatives (104-106) (Fig. 11F). No *lacZ* expression was observed in the endothelial cells of the F10NC transgenic embryos (Fig. 11E and F). In contrast, the 889 bp F10V subfragment directed expression of the transgene only to the endothelium (Fig. 11D). These results clearly show that two separate enhancers in the *mef2c* gene direct the neural crest and endothelial expression patterns.

A Critical 44 Base Pair Element is Conserved After 450 Million Years of Evolution

After separating the neural crest and endothelial enhancers using mouse/chick homology, we reasoned that the critical regulatory elements were contained within the conserved sequence, and we hypothesized that an even smaller region of conservation might exist between more distally related species. Mice and chickens have been separated by approximately 310 million years of evolution, so in an attempt to find a smaller region of conservation, we compared the mouse genome to that of the Japanese pufferfish (*Takifugu rubripes*).

The pufferfish genome has two advantages for use in comparative genomics. The **first** advantage is that mice and pufferfish have been separated by approximately 450 **million** years of evolution, significantly longer than the split between mice and chickens. **The** second reason is that the pufferfish genome is relatively compact compared to other **vertebrates**. While pufferfish and mice both have a similar number of genes, the **pufferfish** genome is almost seven times smaller than the mouse genome, which results in **compression** of noncoding sequences. When we compared the mouse and pufferfish *mef2c* genes, we found a small 44 bp sequence within the 220 bp of mouse/chick **homology** that was 88% conserved between mouse and pufferfish starting at bp 81,169 **and** ending at bp 81,212 of the GS 133 BAC (Fig. 10A). We tested the necessity of this **44** bp sequence by making a construct containing the 5.6 Kb F10 fragment with only the **conserved** 44 bp deleted (5.6 Kb Δ 44) (Fig. 10B). This construct was able to direct **expression** of the transgene to the neural crest, but was unable to direct any expression to **endothelial** cells (Fig. 11G). This result showed that although the 44 bp was necessary for **expression** in endothelial cells, deletion of the 44 bp had no effect whatsoever on **expression** of the transgene in neural crest cells, which further supports the notion that **these** two expression domains are controlled by independent enhancers. We also made a **construct** containing the 889 bp F10V fragment with only the conserved 44 bp deleted (**889** bp Δ 44). This construct was unable to direct expression of the transgene to any **tissue** or cell type within the 9.5 dpc transgenic embryos (Fig. 11H). These constructs **clearly** demonstrate that the 44 bp of mouse/pufferfish conservation is absolutely **nece**ssary for the endothelial expression directed by the *mef2c* endothelial enhancer.

Now that the necessity of the 44 bp conserved element had been shown in vivo, we wanted to test whether this same 44 bp was also sufficient to direct the expression of *lacZ* to the endothelium in vivo. We cloned the 44 bp element into the HSP68-*lacZ* reporter construct (Fig. 10B), and generated transgenic embryos. This 44 bp minimal conserved region directed expression of *lacZ* throughout the entire endothelium (Fig. 11I). This result showed that, in addition to being necessary for endothelial expression, the 44 bp element alone was sufficient to direct expression to the endothelium. This is a potentially exciting result because having a sufficient enhancer that is only 44 bp in length gives us a unique opportunity to identify all of the regulatory elements that are necessary for the endothelial expression directed by this enhancer. With such a small piece of DNA to analyze, we can be very meticulous about analyzing every potential transcription factor binding site and test each one of them either in vitro or in vivo, and potentially both. I believe that we will be able to find all of the regulatory factors that are acting on this enhancer and gain a more complete understanding of how *mef2c*, and presumably other developmentally regulated genes are controlled in endothelial cells.

The 44 bp Enhancer Contains Several Potential Transcription Factor Binding Sites

When we examined the 44 bp enhancer in more detail, we found that it contained several possible binding sites for a number of different transcription factors. Two consensus ETS factor binding sites that are completely conserved between mouse and pufferfish were found within the 44 bp enhancer (Fig. 12). A third, imperfect, consensus ETS factor binding site, which is not completely conserved, was also found within the 44 bp (Fig. 12). We considered these potential ETS sites to be prime candidates for

transcriptional regulator binding sites because ETS factor binding sites have been shown to be necessary for the enhancer or promoter function in several endothelial specific genes, including: *flt-1*, *flk-1*, *Tie*, *Tie-2* (53-56), and *mef2c* itself via a separate endothelial enhancer that we have identified (96).

In addition to the consensus ETS transcription factor binding sites, we also found a consensus E-Box, or bHLH transcription factor binding site within the 44 bp enhancer (Fig. 12), which is also completely conserved between mouse and pufferfish. We believe that this E-Box is a good transcription factor binding site candidate because two E-Boxes that were bound by the bHLH transcription factor SCL/Tal-1 were shown to be necessary for the promoter and enhancer activity of the endothelial gene *flk-1*.

We have also identified a consensus NFAT site (Fig. 12), which is partially conserved between the mouse and pufferfish genomes. NFAT transcription factors are best known for the role they play in the transcriptional regulation of lymphocytes, but NFATs have also been shown to play a role in other tissues such as skeletal muscle, smooth muscle, lung epithelial cells, and the myocardium (107-110). NFAT transcription factors have also been shown to play a role in the regulation of transcription in endothelial cells (111). In addition, based on several lines of evidence including knockouts (4), marker analysis (112), and cell culture colony differentiation studies (6, 10), there is a distinct possibility that hematopoietic and endothelial cells share a common progenitor cell called the hemangioblast.

LIBRARY

RY

UNIVERSITY OF

LIBRARY

LIB

LIB

LIB

LIB

LIB

LIB

LIB

LIB

LIB

LIB

LIB

LIB

LIB

LIB

LIB

LIB

LIB

LIB

LIB

LIB

LIB

LIB

LIB

LIB

LIB

LIB

LIB

LIB

LIB

The Conserved Consensus ETS Binding Sites are Capable of Binding ETS-1

In Vitro

To determine whether the two conserved consensus ETS-binding sites were **functional**, we first tested their ability to bind to a truncated ETS-1 protein in an **electrophoretic mobility shift assay (EMSA)**. We used the truncated ETS-1 protein **known** as $\Delta N336$, which lacks its auto-inhibitory sequence (98), because of reported **difficulties** in performing EMSAs with the full-length ETS-1 protein that contains an **auto-inhibitory** region. We found that both of the conserved ETS-binding sites could bind **to** the truncated $\Delta N336$ ETS-1 in vitro, although the ETS A site bound more strongly than **the** ETS B site (Fig. 13, lanes 4 and 9). This binding was specific to the ETS A and ETS **B** sites as shown by the ability of unlabeled ETS A and ETS B sites to effectively **compete** for ETS-1 binding (Fig. 13, lanes 5 and 10), and the inability of a 100-fold **excess** of unlabeled mutated ETS A and ETS B sites to compete for ETS-1 binding (Fig. **13**, lanes 6 and 11). Furthermore, a 100-fold excess of an unlabeled ETS-binding site **from** the *stromelysin* promoter (113) also effectively competed for ETS-1 binding vs. the **ETS A** and ETS B sites (Fig. 13, lanes 7 and 12). These results demonstrated that both of **the** conserved ETS-binding sites from the 44 bp enhancer are *bona fide* ETS-binding sites **that** can be bound in a specific manner by ETS-1 in vitro.

The Conserved ETS Binding Sites are Necessary for Enhancer Function of the

44 bp Enhancer

Once we determined that the two conserved consensus ETS-binding sites could **bind** to the ETS-1 protein, we wanted to test the necessity of these two sites in vivo using

1917

BY

1917

1917

1917

1917

1917

BY

1917

1917

1917

1917

1917

1917

1917

1917

1917

1917

1917

1917

1917

1917

1917

1917

1917

1917

1917

1917

1917

1917

1917

the transgenic mouse model. We created point mutants in both the ETS A and ETS B **sites** in the context of the entire 5.6 Kb fragment in the HSP68-*lacZ* expression plasmid **and** used this construct to generate transgenic embryos. We created the point mutants in **the** context of the 5.6 Kb fragment so that the neural crest element could serve as an **internal** control for transgene expression. Double mutation of the ETS A and ETS B sites **in** the context of the 5.6 Kb fragment yielded 9.5 dpc embryos that showed strong **exp**ression of *lacZ* in neural crest cells, but no detectable expression in endothelial cells **(Fig. 14D)**. This experiment showed that either the ETS A binding site or the ETS B **binding** site or maybe both are absolutely necessary for the endothelial expression **directed** by this enhancer. To determine which of these two sites are necessary, or **whether** they are redundant in function, we will need to make transgenic mice with each **ETS** site mutated alone. These experiments are currently underway.

The Two Conserved ETS Sites in the 44 bp are Not Sufficient for

Endothelial Enhancer Activity

The results of the ETS site double mutant transgene showed that the function of **the** enhancer was dependent on at least one of the two conserved ETS-binding sites. We **next** tested the sufficiency of these two ETS-binding sites by creating a construct that **cons**isted of three tandem copies of a 44 bp sequence that contained the two conserved **ETS**-binding sites but randomized the remaining 23 bp of the 44 bp enhancer (Fig. 15). **Random**izing this 23 bp of sequence disrupted the non-conserved consensus ETS-binding **site**, the consensus NFAT-binding site, and the conserved consensus E-Box while **keep**ing the ETS A and ETS B binding sites intact (Fig. 15). The nine transgenic embryos

resulting from this construct all showed no expression in any of the endothelial cells throughout the embryo (Fig. 14F), whereas 5 out of 9 transgenic embryos containing a three copy tandem repeat of the wild type 44 bp enhancer directed strong expression to endothelial cells (Fig. 14C). This result showed that the two conserved ETS-binding sites alone are not sufficient for the endothelial enhancer activity of the 44bp enhancer element. Instead, this result shows that there are necessary elements contained within the 23 bp of sequence that was randomized.

As mentioned earlier in this chapter, the conserved E-Box in the 44 bp enhancer was a prime candidate regulatory element binding site. We knew from the previous experiments that the ETS sites alone were not sufficient to direct expression to the endothelium, so we tested the necessity of the E-Box in vivo by mutating the E-Box in the context of the 5.6 Kb fragment and generating transgenic mice. In this preliminary experiment, we obtained a single transgenic embryo that showed strong staining in the neural crest, however, this embryo had a drastic reduction in the expression of *lacZ* in the endothelium (Fig. 14E). Endothelial staining in the trunk, tail, and heart of the embryo was essentially ablated, but endothelial cells in the vasculature of the head were clearly stained. From this embryo, we concluded that the E-Box may be necessary for most of the endothelial expression in the embryo, however, it may not be completely necessary for endothelial staining in the head. We don't know whether this difference in staining reflects a spatial restriction of the function of the E-Box or if it reflects a difference in the strength of the enhancer between the head and the rest of the embryo that becomes apparent when the E-Box is mutated and the levels of endothelial expression are severely reduced throughout the embryo. However, it is clear that the 44 bp of conservation

Index

RY

LIBRARY

C

LIBRARY

LIB

LIBRARY

LIB

between mouse and pufferfish is both necessary and sufficient for endothelial enhancer activity. Furthermore, within this 44 bp regulatory element, the E-Box is important for proper enhancer activity and at least one and maybe both of the conserved ETS-binding sites are necessary for endothelial activity of the enhancer.

Figure 9

The 5.6 Kb F10 fragment directs endothelial and neural crest expression of *lacZ* in transgenic mouse embryos. Expression is first seen at 7.5 dpc (A) in presumptive neural crest cells (NC) in what will become the embryo's head. At 8.0 dpc (B and C) the first endothelial expression can be seen in the yolk sac and the dorsal aortae (DA). At 8.5 dpc (D) the staining can be seen along the entire length of the dorsal aortae and in the endocardium (EC) within the heart. By 9.0 dpc (E) the *lacZ* expression pattern clearly marks the vascular plexus in the yolk sac. At 9.5 dpc (F) staining is seen throughout the entire endothelium, the branchial arches, craniofacial mesenchyme, and dorsal root ganglia (DRG). A transverse section of a 9.5 dpc X-Gal-stained embryo (G) shows *lacZ* expression in the inner endothelial lining of the cardinal veins (CV), the dorsal aortae, the heart, and several smaller blood vessels. Neural crest cells of the branchial arches (BA) can also be seen to stain strongly in this section (G). X-Gal stained vessels dominate the 11.5 dpc transgenic embryo (H), and at 13.5 dpc most of the internal organs are blue due to the abundance of X-Gal stained endothelial cells (I). L, liver; LA, left atrium; LV left ventricle; RA, right atrium; RV, right ventricle

Figure 9

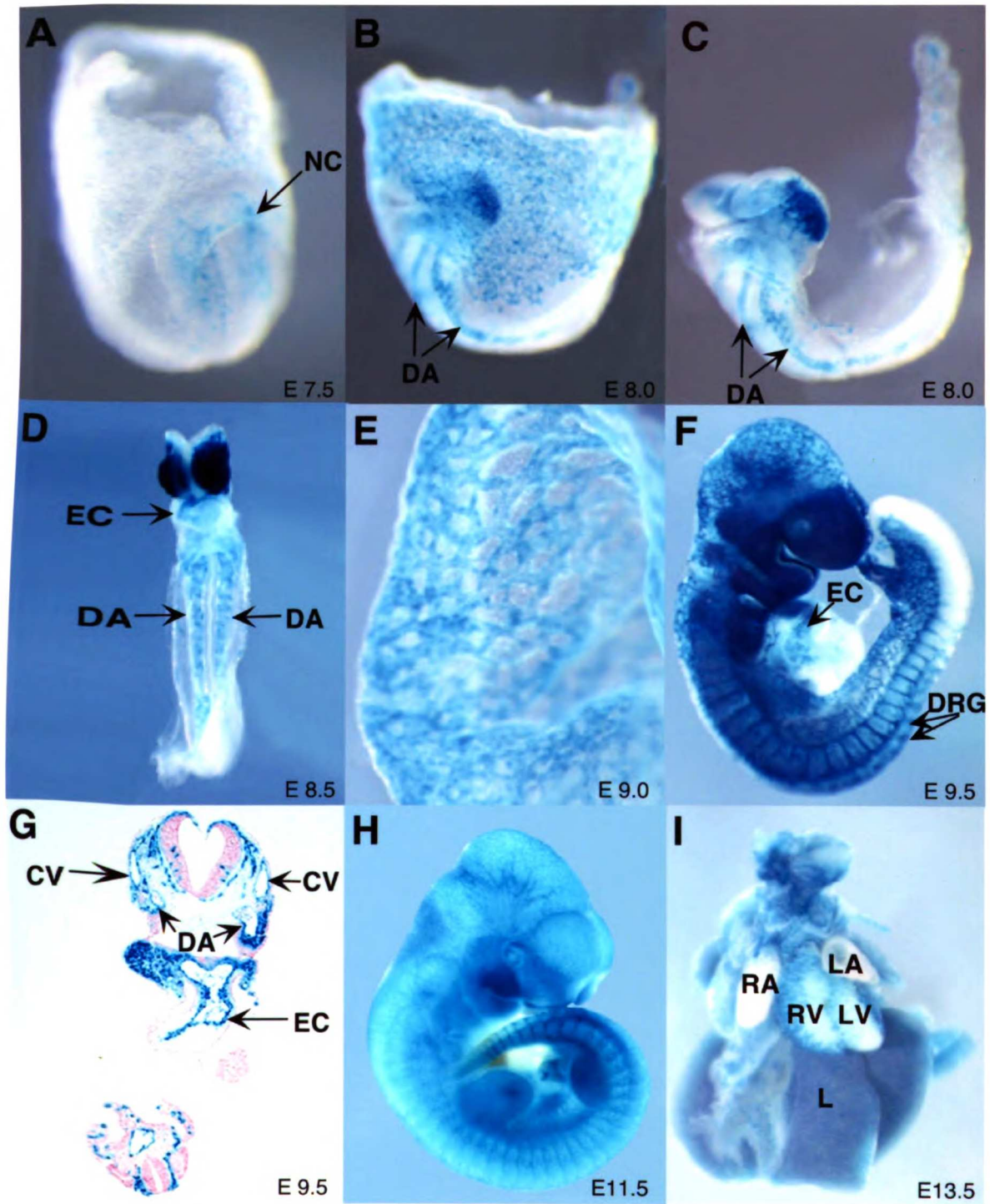
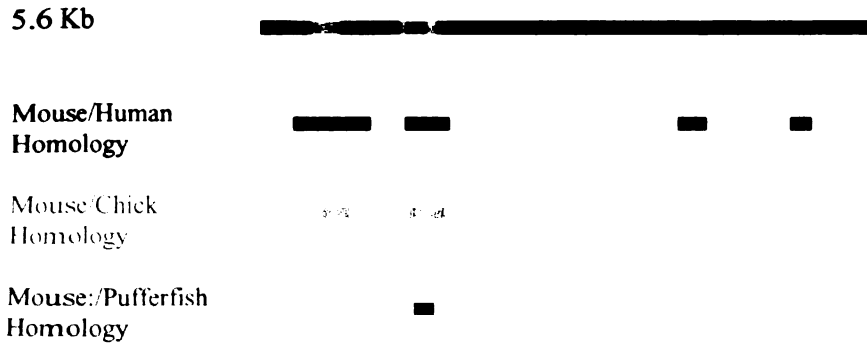


Figure 10

(A) Schematic representation of the evolutionary conservation contained within the 5.6 Kb fragment, which contains a neural crest enhancer and an endothelial enhancer. Mouse/human homology is highlighted in green, mouse/chick homology is highlighted in pink, and mouse/pufferfish homology is highlighted in red. (B) Schematic representations of the *lacZ* transgene constructs used to define the minimal endothelial and neural crest enhancers. Again, mouse/human homology is highlighted in green, mouse/chick homology is highlighted in pink, and mouse/pufferfish homology is highlighted in red. The HSP68 promoter is represented by the blue arrow and the *lacZ* reporter gene is designated in blue.

Figure 10

A



B

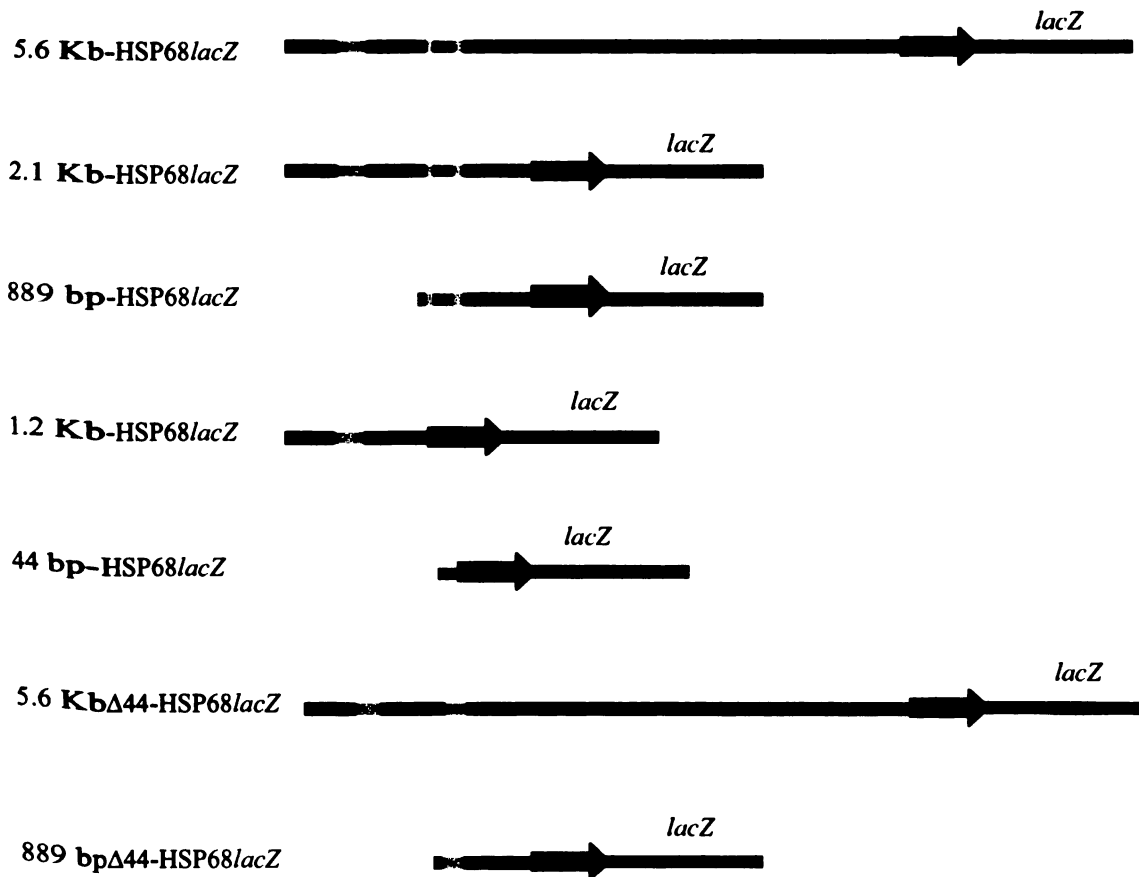


Figure 11

Deletional analysis of the 5.6 Kb fragment revealed two separate enhancers: an endothelial enhancer and a neural crest enhancer. The 120 Kb GS133 *lacZ* transgenic BAC (A) directs expression to all tissues that express *mef2c* including the myocardium (MC) of the heart, the branchial arches (BA), the myotomal compartment of the somites (S), and the vasculature. The full length 5.6 Kb-HSP68*lacZ* construct (B) directed expression to the endothelium and neural crest in five out of six lines tested. The 2.1 Kb-HSP68*lacZ* construct (C) directed expression to the endothelium and neural crest in one out of one line tested. The 889 bp-HSP68*lacZ* construct (D) directed expression only to the endothelium in two out of five lines tested. The 1.2 Kb-HSP68*lacZ* construct (E and F) directed expression to the neural crest including the branchial arches, dorsal root ganglia (DRG) and melanocytes (Me) in four out of eight lines tested. The 5.6 Kb Δ 44-HSP68*lacZ* construct (G) directed expression to the neural crest in seven out of eight lines tested. The 889 bp Δ 44-HSP68*lacZ* construct (H) cannot direct expression to either the endothelium or neural crest in any of the ten lines tested. The 44 bp-HSP68*lacZ* construct (I) directed expression to the endothelium in three out of sixteen lines tested.

Figure 11

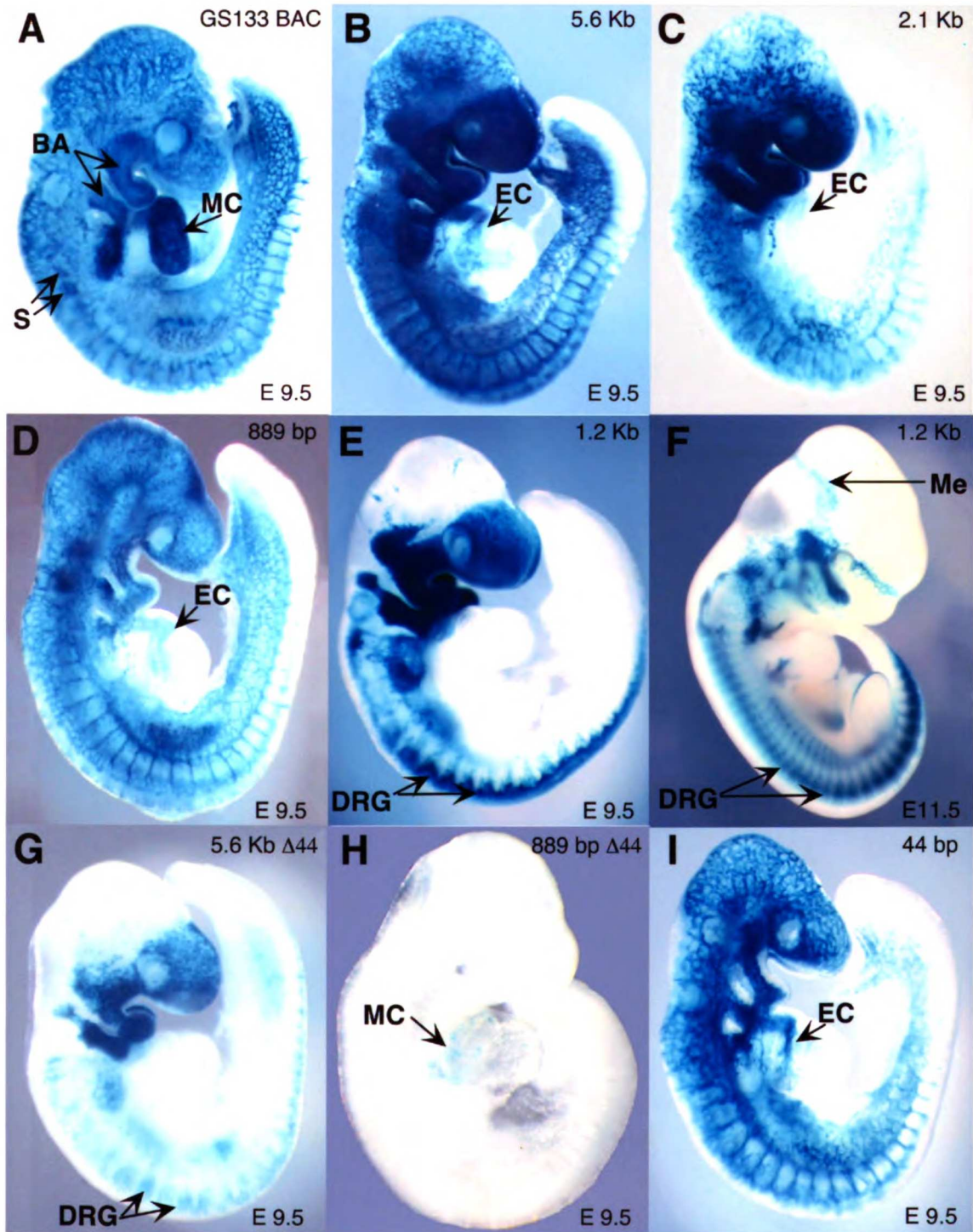


Figure 12

Schematic representation of the 44 bp constructs. (A) The 44 bp of mouse/pufferfish homology includes two conserved consensus ETS-binding sites shown in red (ETS A and ETS B), a conserved consensus bHLH binding site shown in blue (E Box), and a partially conserved consensus NFAT site that could also be an imperfect ETS-binding site shown in green (NFAT/ETS). (B) Each 44 bp module of the 3X 44 bp ETS only construct was created by leaving the conserved ETS A and ETS B sites intact, but randomizing the 23 base pairs of sequence in between (randomized sequence) shown in gray.

Figure 12

A

ETS A NFAT/ETS EBox ETS B



B

ETS A Randomized Sequence ETS B



Figure 13

Electrophoretic mobility shift assays using a truncated ETS-1 protein, which lacks the ETS-1 autoinhibitory region, show that the ETS A and ETS B sites are *bona fide* ETS-binding sites that the ETS-1 protein is capable of binding to. The truncated ETS-1 protein was transcribed and translated in vitro and incubated with radiolabeled double-stranded oligonucleotides representing the control *stromelysin* ETS site (lanes 1 and 2), the conserved ETS A site (lanes 3-7), or the conserved ETS B site (lanes 8-12). ETS-1 efficiently bound to all three sites (lanes 2, 4, and 9). Binding of ETS-1 to the ETS A site was specifically competed by an excess of the unlabeled ETS A probe (lane 5) and by an excess of the unlabeled *stromelysin* ETS site (lane 7), but not by a 100-fold excess of the mutant ETS A site (lane 6). Likewise, Binding of ETS-1 to the ETS B site was specifically competed by an excess of the unlabeled ETS B probe (lane 10) and by an excess of the unlabeled *stromelysin* ETS site (lane 12), but not by a 100-fold excess of the mutant ETS B site (lane 11). In samples where ETS-1 proteins were not included (lanes 1, 3 and 8), an equal amount of unprogrammed reticulocyte lysate was included. Lysate-derived, nonspecific mobility shifts are noted.

Figure 13

	<u>St</u>		<u>Ets A Site</u>					<u>Ets B Site</u>				
ETS-1	-	+	-	+	+	+	+	-	+	+	+	+
competitor	-	-	-	-	A	mA	St	-	-	B	mB	St

lysate →
lysate →

ETS-1 →

probe →

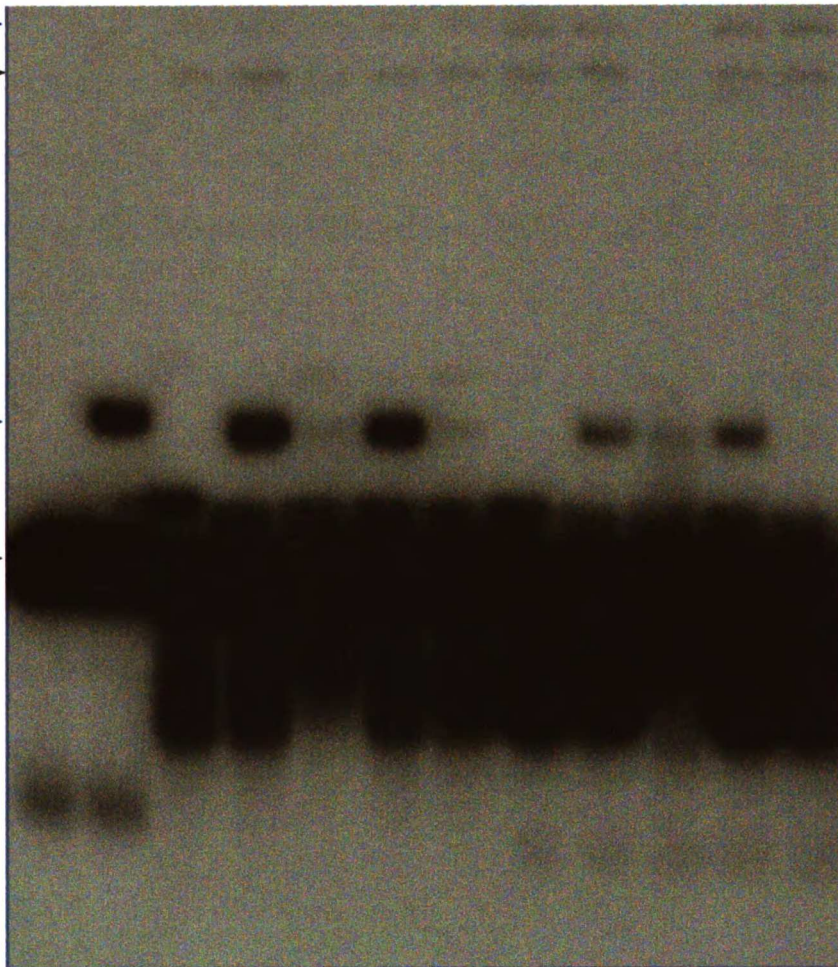


Figure 14

The *mef2c* endothelial enhancer is dependent on ETS and bHLH binding sites for expression in vivo. Representative 9.5 dpc embryos are shown unless otherwise indicated. The wild type full-length 5.6 Kb fragment directs expression to neural crest cells of the branchial arches, craniofacial mesoderm, and DRGs as well as to the entire endothelium (A). We mutated the ETS sites and E-Box in the context of this full 5.6 Kb fragment so that the neural crest expression pattern directed by the 1.2 Kb neural crest enhancer (B) would serve as an internal positive control for transgene expression. Mutation of both conserved ETS-binding sites (ETS A/Bmut) completely eliminated endothelial expression (D). Mutation of the conserved E-Box (E-Box mut) eliminated most of the endothelial expression, especially expression in the trunk and tail (E). A construct consisting of three tandem repeats of the wild type 44 bp enhancer cloned into the HSP68-*lacZ* reporter plasmid (3X 44 bp) directs exceedingly strong expression to the endothelium in five out of nine transgenic lines tested (C). However, randomization of the 23 base pairs between the two conserved ETS-binding sites in the context of the same triple repeat in the HSP68-*lacZ* plasmid (3X 44bp ETS only) resulted in nine separate transgenic lines, none of which expressed *lacZ* in the endothelium (F). The embryo with the most β -Gal staining out of the nine lines is shown.

Figure 14

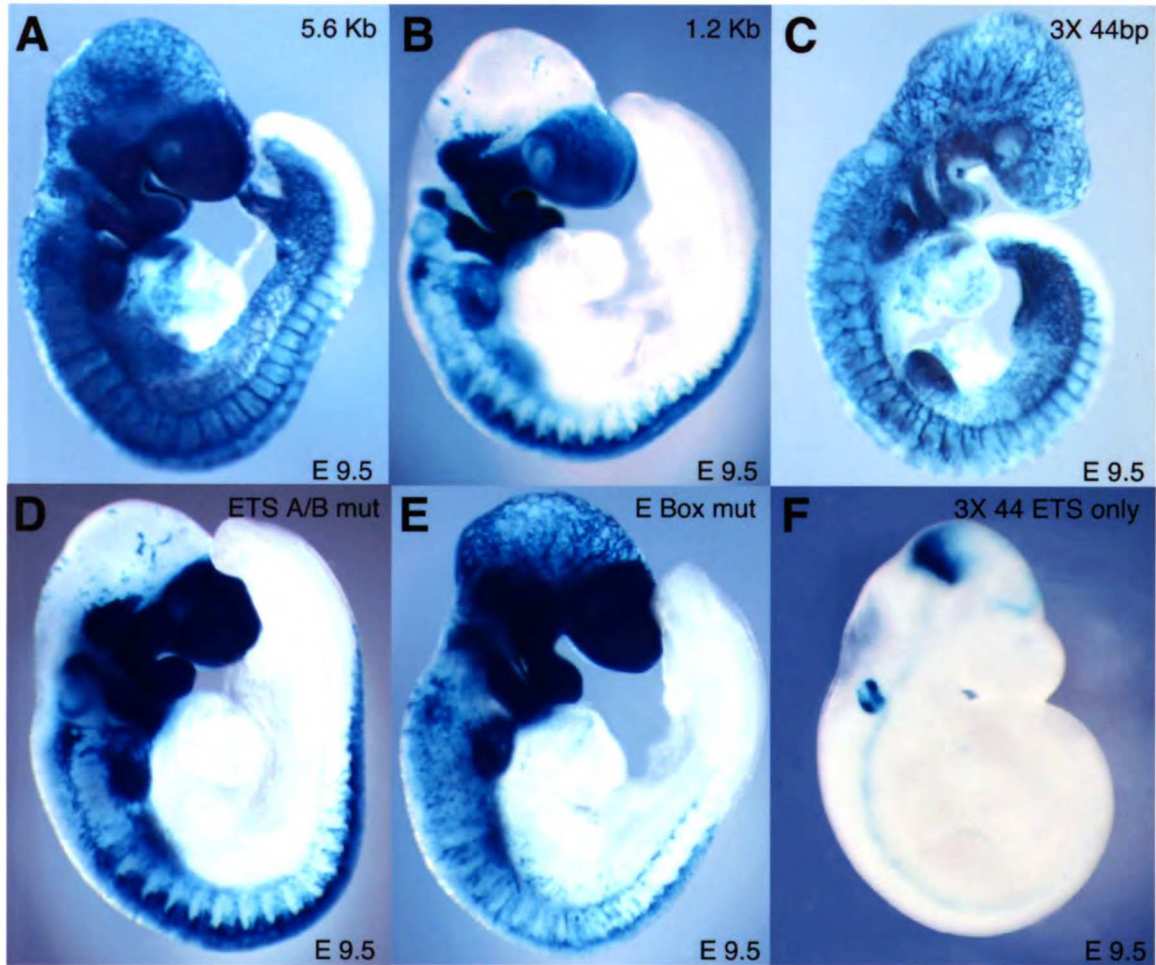


Figure 15

Schematic representations of the 44 bp constructs used to define the minimal sufficient endothelial enhancer. (A) The 44 bp of sequence that was conserved between mouse and pufferfish was cloned into the HSP68*lacZ* reporter plasmid alone and was sufficient to direct expression to the endothelium. (B) In order to make the 3X 44 bp ETS only construct, the conserved ETS A and ETS B sites were left intact, but the 23 base pairs of sequence between the two sites were randomized; destroying the E-Box, NFAT/ETS site, and any other regulatory sequences that may have existed between the two conserved ETS sites. Three tandem repeats of this 44 bp sequence were cloned upstream of the HSP68*lacZ* reporter plasmid to make the 3X 44 bp ETS only construct.

Figure 15

A 44 bp-HSP68*lacZ*



B 3X 44 bp ETS only-HSP68*lacZ*



Chapter 5

Future Directions

Investigating the Regulation and Function of *Mef2c* in Vascular Smooth Muscle

Before I began my research on the transcriptional pathways involving the *mef2c* gene during vascular development, we knew close to nothing about the role of MEF2C in either smooth muscle or endothelial cells. We now know that a MEF2 transcription factor is necessary for expression of the *HRC* gene in arterial smooth muscle and that a 44 bp enhancer that contains two necessary ETS-binding sites and a necessary E-Box regulates endothelial expression of *mef2c*. However, there is still a lot that we do not know. For instance, how is *mef2c* regulated in vascular smooth muscle? In our search for regulatory elements using evolutionary conservation we discovered several tissue-specific enhancers, but we did not identify a smooth muscle enhancer. We are still looking for smooth muscle enhancers from the *mef2c* gene, especially now that a transcriptional target for MEF2C has been identified in arterial smooth muscle.

We would also like to find other targets of MEF2C in vascular smooth muscle cells now that *HRC* has been identified as a *bona fide* target. While the vast majority of smooth muscle genes studied so far have been shown to be transcriptionally regulated by the MEF2-related transcription factor SRF, most of these genes are part of the contractile complex, for example: *SM22 α* and *smooth muscle alpha actin* (114-117). The *HRC* gene however, is not a part of the contractile complex. Although we do not yet know the true function of HRCBP, we believe that it plays a role in calcium handling in smooth muscle, and it will be interesting to see if other proteins involved in calcium uptake and release, such as the ryanodine receptor, are also regulated by MEF2 and not SRF.

Searching for a MEF2 Target in Endothelial Cells

While we now know of at least one target of MEF2 transcription factors in smooth muscle, we still do not know what the exact role of MEF2 is in endothelial cells. Based on the role of MEF2 factors in cardiac and skeletal muscle, we assume that MEF2C and possibly other MEF2 factors are serving as transcriptional activators of a number of endothelial-specific genes necessary for the function of differentiated endothelial cells. However, nobody has yet described a MEF2 target in endothelial cells. Before we can truly know what MEF2C is doing in endothelial cells, we will have to discover which genes it is controlling the expression of, when it is turning these genes on, and what the effects of this transcriptional regulation are on endothelial cells. This is why it is important to discover MEF2 targets in endothelial cells. One possible way to identify such targets would be to culture human umbilical vein endothelial cells (HUVECs) and transfect them with a *mef2c* expressing plasmid. We could use a microarray to compare *mef2c*-transfected HUVECs with empty vector-transfected HUVECs and look for genes that are upregulated upon *mef2c* transfection. We would then look for conserved MEF2 sites in likely promoters and enhancers in genes that look like promising candidates and follow the same methodology that we used to identify *HRC* as the first vascular smooth muscle MEF2 target in Chapter 2.

Defining All of the Transcriptional Regulators From the 44 bp Enhancer

In this dissertation, I have described how we defined a necessary and sufficient 44 bp *mef2c* endothelial enhancer. We then identified within this minimal enhancer two conserved ETS-binding sites that, if mutated simultaneously, completely ablated the

ability of the enhancer to direct expression to endothelial cells. We also identified a conserved E-Box within the 44 bp enhancer, which we found was necessary for most of the endothelial expression directed by the enhancer. In addition to these three sites, we have identified a consensus NFAT-binding site that could also be an imperfect ETS-binding site. These sites are not completely conserved between mouse and pufferfish, and we have not yet determined whether they are necessary for enhancer function. So, while we have found a very small minimal enhancer and a few necessary transcription factor binding sites, many questions remain to be addressed in order to fully define the transcriptional regulation of the *mef2c* gene in endothelial cells.

First, we have to test each of the conserved ETS-binding sites in vivo to determine which of the two sites are necessary, if both are necessary, or if both sites are partially necessary. Once we determine which ETS sites are truly necessary, we will then want to determine which ETS transcription factor is binding to the site and is responsible for the regulation of transcription. Likewise, we still do not know which bHLH transcription factor is binding to the E-Box and regulating transcription, or if the E-Box is even functional. To determine the specific transcription factors that are binding to our necessary binding sites, we are currently performing an EMSA analysis of all of these sites, but quite often, several transcription factors in a family will bind the same site in an EMSA. In addition, EMSAs are in vitro assays, which may not give us a completely accurate picture of what is happening in vivo. Specific transcription factors could also be identified in co-transfection studies where different transcription factors are expressed in 10T1/2 fibroblasts co-transfected with the 44 bp enhancer in a reporter plasmid. In these studies, one can measure the activation potential of several transcription factors relative

to a specific enhancer. Cell culture experiments are a little closer to representing what is happening in vivo, but still cannot take into account many of the variables that exist in a living animal.

Another method that would help us understand which particular factors are regulating transcription is Chromatin Immunoprecipitation (ChIP). ChIP is a technique that can be used to determine whether a specific transcription factor is bound to a specific genomic location in vivo. This technique could be useful because we could test a number of different ETS and bHLH proteins to discover which particular ETS and bHLH family members are bound to the 44 bp enhancer in vivo. ChIP could also potentially tell us if any of the NFAT proteins can bind the 44 bp enhancer, and thereby settle the issue of what kind of transcription factor is binding at the partially conserved NFAT/ETS-binding site. However, we still haven't determined whether this site really is important for enhancer function in vivo. We are currently testing the necessity of the NFAT/ETS-binding site by making a mutation in this site that would disrupt both NFAT and ETS factor binding in the context of the 5.6 Kb fragment and testing the enhancer activity in transgenic mouse embryos.

Although we have looked very carefully at the 44 bp sequence and believe that we have found all of the important known transcription factor binding sites contained within this minimal enhancer, we still cannot rule out the possibility that there are some as yet unknown transcription factor binding sites in the 44 bp. To address this issue and potentially find novel transcription factor binding sites, we are currently performing a Yeast-One-Hybrid screen, using a three-copy tandem repeat of the 44 bp element as bait and a 9.5 dpc cardiac library (including endocardium) as prey. In the Yeast-One-Hybrid

experiment we seek to identify every transcription factor that binds to the 44 bp element, whether or not the binding site for the factor is known. In addition, for proteins like the ETS factors, the Yeast-One-Hybrid could tell us which specific family members are regulating endothelial expression, something that cannot be known by the binding site sequence alone.

Importance of a Completely Defined Endothelial Enhancer

As mentioned earlier in this chapter, we are currently trying to find every transcription factor that binds to the 44 bp enhancer and plays a role in regulating expression of the *mef2c* gene in endothelial cells. By discovering a necessary and sufficient enhancer that is only 44 bp in length, we feel that we are in a unique position to discover all of the regulatory elements that are playing a role through this endothelial enhancer. This is an exciting prospect for two reasons. First, by defining all of the regulatory elements necessary for directing expression of *mef2c* to the endothelium, we will have the most complete picture of how an endothelial gene is regulated to date. Using all of the techniques I have outlined above, in conjunction with such a small enhancer to search, we should be able to define all of the necessary transcription factors involved and use this knowledge to better understand the entire transcriptional complex for this enhancer.

The second reason that we are excited by the prospect of finding all of the necessary regulatory elements for the endothelial enhancer is because there is the possibility that the 44 bp enhancer contains a particular combination of binding sites that may be present in the enhancers of other developmental endothelial genes. Once we

determine the exact combination of transcription factors necessary for the 44 bp enhancer activity, we can look at other known endothelial genes and try to find the same combination of binding sites in their enhancers. In addition, we hope to create an algorithm that will be able to search the mouse genome for this same combination of binding sites even if they do not appear in the same exact order as they do in the 44 bp element. In this way, we will attempt to discover new endothelial genes and new roles in the endothelium for some already well-known genes.

Materials and Methods

Cloning, Plasmids, and Mutagenesis.

A 2,726-bp fragment of the human *HRC* gene encompassing the region from —2609 to +117 relative to the transcriptional start site was subcloned from a lambda GT10 genomic library as a Sall-Psp1406I fragment into Sall-ClaI-cleaved pBluescript SKII(+), using standard techniques. The resulting product was further subcloned into the promoterless *lacZ* reporter plasmid AUG- β -gal (118) to create the plasmid *HRC-lacZ* for generation and analysis of transgenic mice and for transfection analyses. The 2,726-bp product was also subcloned into pCAT-Basic (Promega) to create plasmid *HRC-CAT* for transfection analyses comparing expression in fibroblasts, myoblasts, and myotubes. The *myogenin* promoter and enhancer (—1565 to +18) cloned into plasmid pCAT-Basic to create plasmid pMYO1565CAT has been described elsewhere (81). A 3.8-kb fragment of the mouse *smooth muscle α -actin* (*SMaa*) promoter and enhancer, including 1.1 kb of upstream sequence and 2.7 kb from the first intron, was amplified from genomic DNA using the primers *SMaa* forward and *SMaa* reverse (Table 1). This fragment was confirmed by sequencing and was cloned into plasmid AUG- β -gal for transfection analyses. This construct is nearly identical to the rat *SMaa* promoter and enhancer, which has been described previously (116). The expression plasmids pCDNA1.MEF2A and pCDNA1.MEF2C are also described elsewhere (119). Plasmid pCGN.SRF contains the mouse SRF cDNA under control of the cytomegalovirus promoter (120). The MEF2 mutation in the *HRC* enhancer was generated using the PCR mutagenesis technique of gene splicing by overlap extension (gene SOEing) (121) to create the mutant sequence:

HRC MEF2 mut (Table 3) in the context of the full-length 2,726-bp *HRC* fragment. The entire sequence of the mutant fragment was confirmed by sequencing on both strands. The GenBank accession numbers for the sequences of the human and mouse *HRC* enhancers are AY321454 and AY321455, respectively.

A 5,550-bp fragment of the mouse *mef2c* gene from within intron 5 (F10) was PCR-amplified from bp 77,569 to bp 83,118 of the GS133 BAC with *Xma*I restriction sites engineered into both ends of the PCR product (Table 1). This 5.6 Kb fragment, was cloned as an *Xma*I fragment into an *Xma*I-cleaved pBluescript SKII(+) plasmid, using standard techniques. The resulting product was then subcloned into the transgenic reporter plasmid HSP68-*lacZ* (94) for generation and analysis of transgenic mice. Mutations were introduced into the wild-type 5.6 Kb endothelial enhancer fragment by PCR gene SOEing as described above to create mutant sequences within the context of the 5.6 Kb fragment (Table 3). The sequence of each mutant fragment was confirmed by sequencing on both strands. The 2.1 Kb, 1.2 Kb, and 889 bp subfragments were generated by various restriction digests of the 5.6 Kb fragment and also cloned into the HSP68-*lacZ* reporter plasmid. The 44 bp, 3X 44 bp and 3X ETS only 44 bp constructs were created by annealing complementary primers with overhangs at both ends to facilitate cloning into the HSP68-*lacZ* reporter plasmid. The primers used to make these constructs are found in Table 2.

Fragments 1-7 and 9 were PCR-amplified from the GS 133 BAC with primers engineered to create either *Xma*I sites or *Xho*I and *Sal*I sites at the ends of the PCR-amplified fragments (Table 1). The fragments with *Xma*I sites at their ends were first cloned into an *Xma*I-cleaved pBluescript SKII(+) plasmid, and then subcloned into an

XmaI-cleaved HSP68-*lacZ* transgenic reporter plasmid. The fragments with a XhoI site at one end and a Sall site at the other were first cloned into a XhoI/Sall-cleaved pBluescript SKII(+) plasmid, and then subcloned into an XhoI-cleaved HSP68-*lacZ* transgenic reporter plasmid, leaving the XhoI site at the 5' end intact, but destroying the XhoI and Sall sites at the 3' end.

Generation of Transgenic Mice

Transgenic reporter fragments were digested and gel purified using standard techniques and were suspended in 5 mM Tris-Cl, 0.2 mM EDTA (pH 7.4) at a concentration of 2 ng/1 for pronuclear injection as described previously (83). Injected embryos were implanted into pseudopregnant CD-1 females, and embryos were collected at indicated time points for transient analysis or were allowed to develop to adulthood for establishment of stable transgenic lines. DNA was extracted from the yolk sac and amnion of embryos or from tail biopsies from mice by digestion in tail lysis buffer (100 mM NaCl, 25 mM EDTA, 1% sodium dodecyl sulfate, 10 mM Tris-Cl, 200 g of proteinase K/ml; pH 8.0) at 56°C overnight. Digested samples were extracted once with phenol-chloroform and ethanol precipitated. DNA preparations were digested with EcoRV and analyzed by Southern blotting using a radiolabeled *lacZ* probe. All experiments using animals complied with federal and institutional guidelines and were reviewed and approved by the UCSF Institutional Animal Care and Use Committee.

X-Gal Staining and Immunohistochemistry

β -Galactosidase expression from *lacZ* transgenic embryos, embryonic tissues, and adult tissues was detected by 5-bromo-4-chloro-3-indolyl- β -D-galactopyranoside (X-Gal) staining as described previously (95). Some embryos were dehydrated in ethanol and cleared for 1 to 3 h in a 1:1 mixture of benzyl alcohol and benzyl benzoate prior to photography for better visualization of staining under the skin. For transverse sections, embryos were collected at either 9.5 or 11.5 days postcoitum (dpc), fixed, and stained with X-Gal. Following staining, the embryos were fixed in 4% paraformaldehyde in phosphate-buffered saline (PBS), rinsed, and dehydrated with a series of ethanol washes (70 to 100%) followed by three brief washes in xylene. Samples were then mounted in paraffin, and transverse sections were cut at a thickness of 5 μ m using a Leica RM 2155 microtome and mounted on glass slides. Sections were counterstained with Nuclear Fast Red to visualize embryonic structures. For antibody staining, embryos were collected, fixed, and sectioned as described above. The sections were rehydrated through a series of ethanol washes (100 to 70%) and then were placed in PBS for 5 min. The sections were then blocked for 20 min in 3% normal goat serum diluted in PBS. Incubation in both primary antibodies was performed concurrently for 1 h at room temperature in a humid chamber. Mouse monoclonal anti-skeletal muscle myosin (MY-32; Sigma) and rabbit anti- β -galactosidase (ICN) were diluted 1:300 in 3% normal goat serum. Following incubation with the primary antibodies, the sections were washed three times for 10 min each with PBS. The secondary antibodies, Oregon Green-conjugated goat anti-rabbit (Molecular Probes) and tetramethyl rhodamine isocyanate (TRITC)-conjugated anti-mouse (Sigma), were diluted 1:300 into 3% normal goat serum and incubated for 1 h at

room temperature in a humid chamber in the dark, followed by three washes in PBS. Slides were mounted using a SlowFade Light antifade kit (Molecular Probes) and photographed on a fluorescence microscope.

Cell Culture, Transfections, and Reporter Assays

C3H10T1/2 (10T1/2) cells were maintained in Dulbecco modified Eagle medium (DMEM) supplemented with 10% fetal calf serum. C2C12 myoblasts were maintained in DMEM plus 15% fetal calf serum. For generation of myotubes, C2C12 cells were maintained in DMEM plus 2% horse serum as described previously for the transfection of myotubes (122). Transfections were performed by calcium phosphate precipitation in 60-mm-diameter dishes as described elsewhere (95). In transfections of the reporter plasmid only into 10T1/2 cells, C2C12 myoblasts, and C2C12 myotubes, 10 μ g of the *HRC-CAT* reporter (—2609 to +117), the *myogenin-CAT* reporter (pMYO1565CAT), pCAT-Basic (Promega), or a constitutively active simian virus 40 (SV40)-CAT plasmid were used. Within each cell type, transfections were normalized as described previously (122). To account for differences in transfection efficiencies between the different cell types, the activity of SV40-CAT was set to 100% in each set of transfections for each cell type, and the data are expressed as a percentage of the activity obtained with SV40-CAT in that cell type. The activity of SV40-CAT is roughly equivalent among the three cell types used in these studies when normalized for transfection efficiency (122). For *trans*-activation analyses, 5 μ g of *HRC-lacZ* or the *SMAa-lacZ* reporter was transfected along with either 5 μ g of pCDNA1.MEF2A, 5 μ g of pCDNA1.MEF2C, or 5 μ g of pCDNA1.SRF expression

plasmid by calcium phosphate precipitation. In samples where a cDNA expression plasmid was not transfected, an equal amount of the parental pCDNA1/amp expression vector (Invitrogen) was transfected. For chloramphenicol acetyltransferase (CAT) assays, transfected cells were harvested, and cellular extracts were prepared by sonication, heat inactivated, and normalized as described previously (123). CAT activity was determined as described previously (124). Reactions were conducted for 5 h at 37°C. Conversion to acetylated forms was analyzed by thin-layer chromatography and quantitated by phosphorimager analysis (Molecular Dynamics, Inc.). For β -galactosidase assays, transfected cells were harvested and cellular extracts were prepared by sonication and normalized as described previously (95). Chemiluminescent β -galactosidase assays were performed using the luminescent β -gal kit (Clontech) according to the manufacturer's recommendations, and relative light units were detected using a Tropic TR717 microplate luminometer (PE Applied Biosystems).

Electrophoretic Mobility Shift Assays

DNA-binding reactions were performed as described previously (95). Briefly, double-stranded oligonucleotides for use in binding reactions were labeled with (³²P)dCTP using Klenow to fill in overhanging 5' ends and purified on a non-denaturing polyacrylamide-Tris-borate-EDTA gel. Binding reactions were preincubated at room temperature in 1x binding buffer (40 mM KCl, 15 mM HEPES [pH 7.9], 1 mM EDTA, 0.5 mM dithiothreitol, 5% glycerol) containing 2 μ g of reticulocyte lysate containing recombinant MEF2A, SRF, or ETS-1 protein or 2 μ g of unprogrammed reticulocyte

lysate, 1 g of poly (dI-dC), and competitor DNA (100-fold excess where indicated) for 10 min prior to probe addition. Recombinant MEF2A, SRF, and Δ N336ETS-1 proteins were generated from plasmid pCDNA1.MEF2A, plasmid pCDNA1.SRF, and plasmid pCITE2. Δ N336ETS-1 by transcribing with T7 polymerase and translating in vitro using the TNT Quick coupled transcription-translation system as described in the manufacturer's directions (Promega). Reaction mixtures were incubated an additional 20 minutes at room temperature after probe addition and electrophoresed on a 6% nondenaturing polyacrylamide gel. The oligonucleotides for the myogenin MEF2 site and a mutant form of that site have been described previously (82). The oligonucleotides for the SMaa intronic CArG box and a mutant form of that site have also been described previously (116). The sense-strand sequences of the oligonucleotides used for electrophoretic mobility shift assays (EMSAs) are found in Table 3. The *stromelysin* ETS-1 control wild-type and mutant binding site oligonucleotides were adapted from previously described sequences (113) and the sense strand sequences can be found in Table 3.

Table 1: Primer Sequences

SMaa forward: 5'-ACACCATAAAACAAGTGCATGAGC-3'
SMaa reverse: 5'-GCAGCGTCTCAGGGTTCTGCA-3'
F1 forward: 5'-AGTGGGAAGCATAAGGCCCGGGAAGTCTGAT-3'
F1 reverse: 5'-ATGGTACCGTGTATGGTGGTCCCAGGAATGT-3'
F2 forward: 5'-CATAGATATGACTCGAGGTGACTTGAATTGAATTG-3'
F2 reverse: 5'-AGGATGAGGTCGACTATAAATATTTGCTTTAGAAC-3'
F3 forward: 5'-TTTGCCTATGATTACTTTGTCCCAGGTTATTC-3'
F3 reverse: 5'-AAGGTGATTGTCTCTATAAAGCCCGGATTGTA-3'
F4 forward: 5'-CTATTGGTCAGAAGGAAGATCTCGAGTTCAGAAG-3'
F4 reverse: 5'-CTAGGCAAATTTCCCTTATATTTATGTCGACAAA-3'
F5 forward: 5'-TAAAAAACAGACCCCCCTCGAGACTCCACCAGCG-3'
F5 reverse: 5'-TACTATAATGTAGAAGATACAAGAGTCGACAATA-3'
F6 forward: 5'-AAGCCACCAGTTTCTTTGTCTCGAGGTATTTAT-3'
F6 reverse: 5'-TTACCTGCCATGCACTTGCTTTAGGTCGACTTT-3'
F7 forward: 5'-CTTTCAAACAAACCCGGGAGTAGAAAG-3'
F7 reverse: 5'-AGCCAGTTTCCCAGGTTTCATCAGG-3'
F9 forward: 5'-TTGATTCCCAGGTGATGAGTCTA-3'
F9 reverse: 5'-GGTTTTCTTCCCAGGTTTCTCC-3'
F10 forward: 5'-CATCTCCTTTTCCCAGGTTTCC-3'
F10 reverse: 5'-CCTTCTCCCAGGCCCATCTCTGT-3'

Table 2: 44bp Oligonucleotide Sequences

44bp CI for: 5'-TCGAGCAGGAAGCACATTTGTCTACGCTTTCCTGTCATAACAGGAAGAGA-3'

44bp CI rev: 5'-AGCTTCTCTTCCTGTTATGACAGGAAAGCGTAGACAAATGTGCTTCCTGC-3'

44bp CII for: 5'-AGCTTCAGGAAGCACATTTGTCTACGCTTTCCTGTCATAACAGGAAGAGCTGCA-3'

44bp CII rev: 5'-GCTCTTCCTGTTATGACAGGAAAGCGTAGACAAATGTGCTTCCTGA-3'

44bp CIII for: 5'-GCAGGAAGCACATTTGTCTACGCTTTCCTGTCATAACAGGAAGAGC-3'

44bp CIII rev: 5'-CCGGGCTCTTCCTGTTATGACAGGAAAGCGTAGACAAATGTGCTTCCTGCTGCA-3'

ETS only 44bp CI for: 5'TCGAGCAGGAAGCAT**TGTAACCGCAGAGATGCCAGTTAT**TAACAGGAAGAGA-3'

ETS only 44bp CI rev: 5'-AGCTTCTCTTCCTGTTA**AATAACTGCATCTCTGCCGOTTACA**TGCTTCCTGC-3'

ETS only 44bp CII for:

5'-AGCTTCAGGAAGCAT**TGTAACCGCAGAGATGCCAGTTAT**TAACAGGAAGAGCTGCA-3'

ETS only 44bp CII rev: 5'-GCTCTTCCTGTTA**AATAACTGCATCTCTGCCGOTTACA**TGCTTCCTGA-3'

ETS only 44bp CIII for: 5'-GCAGGAAGCAT**TGTAACCGCAGAGATGCCAGTTAT**TAACAGGAAGAGC-3'

ETS only 44bp CIII rev:

5'-CCGGGCTCTTCCTGTTA**AATAACTGCATCTCTGCCGOTTACA**TGCTTCCTGCTGCA-3'

Table 3: Mutant and EMSA Sequences

Point Mutant Sequences:

HRC MEF2 mut 5'-CCTCCGAGCTGGATCCTCCGCCCTGGCCTAG-3'

ETS A point mutant: 5'-AGTTACTCTCTTCTAGATATGACA-3'

ETS B point mutant: 5'-CAAATGTGGGCCCTGAGTTAGCT-3'

ETS A/B point mutant:

5'-AGTTACTCTCTTCTAGATATGACAGGAAAGCGTAGACAAATGTGGGCCCTGAGTTAGCT-3'

E-Box point mutant: 5'-AAAGCGTAGATCTATGTGCTTCCTGAGTTAG-3'

EMSA sense-strand sequences:

wild-type MEF2 site, 5'-TCCCAGCTGTATTTATAGCCCTGGCCTAGCCCA-3';

mutant MEF2 site, 5'-TCCCAGCTGGATCCTCCGCCCTGGCCTAGCCCA-3';

wild-type ETS A site, 5'-AGTTACTCTCTCCTGTTATGACA -3';

mutant ETS A site, 5'- AGTTACTCTCTTCTAGATATGACA -3';

wild-type ETS B site, 5'-CAAATGTGCTTCCTGAGTTAGCT -3';

mutant ETS B site, 5'-CAAATGTGGGCCCTGAGTTAGCT -3'.

wild-type *stromelysin* ETS site, 5'-GTCGAGCAGGAAGCATTTCCTGGTCA-3';

mutant *stromelysin* ETS site, 5'-GTCGAGCAACAAGCATTTCCTGGTCA-3'.

Bibliography

1. NCIPC. 2002. WISQARS Leading Causes of Death Reports. Atlanta, GA: Centers for Disease Control and Prevention.
2. Kaufman, M.H. 1994. *Atlas of Mouse Development*. San Diego, CA: Harcourt Brace and Company. 59 pp.
3. Moore, K.L., and Persaud, T.V.N. 1993. *The Developing Human: Clinically Oriented Embryology*. Philadelphia, PA: W.B. Saunders Co. 312 pp.
4. Shalaby, F., Rossant, J., Yamaguchi, T.P., Gertsenstein, M., Wu, X.F., Breitman, M.L., and Schuh, A.C. 1995. Failure of blood-island formation and vasculogenesis in Flk-1-deficient mice. *Nature* 376:62-66.
5. Fong, G.H., Rossant, J., Gertsenstein, M., and Breitman, M.L. 1995. Role of the Flt-1 receptor tyrosine kinase in regulating the assembly of vascular endothelium. *Nature* 376:66-70.
6. Choi, K., Kennedy, M., Kazarov, A., Papadimitriou, J.C., and Keller, G. 1998. A common precursor for hematopoietic and endothelial cells. *Development* 125:725-732.
7. Risau, W. 1997. Mechanisms of angiogenesis. *Nature* 386:671-674.
8. Carmeliet, P., Ferreira, V., Breier, G., Pollefeyt, S., Kieckens, L., Gertsenstein, M., Fahrig, M., Vandenhoek, A., Harpal, K., Eberhardt, C., et al. 1996. Abnormal blood vessel development and lethality in embryos lacking a single VEGF allele. *Nature* 380:435-439.
9. Ferrara, N., Carver-Moore, K., Chen, H., Dowd, M., Lu, L., O'Shea, K.S., Powell-Braxton, L., Hillan, K.J., and Moore, M.W. 1996. Heterozygous embryonic lethality induced by targeted inactivation of the VEGF gene. *Nature* 380:439-442.
10. Eichmann, A., Corbel, C., Nataf, V., Vaigot, P., Breant, C., and Le Douarin, N.M. 1997. Ligand-dependent development of the endothelial and hemopoietic lineages from embryonic mesodermal cells expressing vascular endothelial growth factor receptor 2. *Proc Natl Acad Sci U S A* 94:5141-5146.
11. Pardanaud, L., Altmann, C., Kitos, P., Dieterlen-Lievre, F., and Buck, C.A. 1987. Vasculogenesis in the early quail blastodisc as studied with a monoclonal antibody recognizing endothelial cells. *Development* 100:339-349.
12. Hirakow, R., and Hiruma, T. 1981. Scanning electron microscopic study on the development of primitive blood vessels in chick embryos at the early somite-stage. *Anat Embryol (Berl)* 163:299-306.
13. Oettgen, P. 2001. Transcriptional regulation of vascular development. *Circ Res* 89:380-388.

14. Vikkula, M., Boon, L.M., Carraway, K.L., 3rd, Calvert, J.T., Diamonti, A.J., Goumnerov, B., Pasyk, K.A., Marchuk, D.A., Warman, M.L., Cantley, L.C., et al. 1996. Vascular dysmorphogenesis caused by an activating mutation in the receptor tyrosine kinase TIE2. *Cell* 87:1181-1190.
15. Hirakow, R., and Hiruma, T. 1983. TEM-studies on development and canalization of the dorsal aorta in the chick embryo. *Anat Embryol (Berl)* 166:307-315.
16. Folkman, J., and D'Amore, P.A. 1996. Blood vessel formation: what is its molecular basis? *Cell* 87:1153-1155.
17. Flamme, I., Frolich, T., and Risau, W. 1997. Molecular mechanisms of vasculogenesis and embryonic angiogenesis. *J Cell Physiol* 173:206-210.
18. Shweiki, D., Itin, A., Soffer, D., and Keshet, E. 1992. Vascular endothelial growth factor induced by hypoxia may mediate hypoxia-initiated angiogenesis. *Nature* 359:843-845.
19. Plate, K.H., Breier, G., Weich, H.A., and Risau, W. 1992. Vascular endothelial growth factor is a potential tumour angiogenesis factor in human gliomas in vivo. *Nature* 359:845-848.
20. Semenza, G.L., Jiang, B.H., Leung, S.W., Passantino, R., Concordet, J.P., Maire, P., and Giallongo, A. 1996. Hypoxia response elements in the aldolase A, enolase 1, and lactate dehydrogenase A gene promoters contain essential binding sites for hypoxia-inducible factor 1. *J Biol Chem* 271:32529-32537.
21. Burbach, K.M., Poland, A., and Bradfield, C.A. 1992. Cloning of the Ah-receptor cDNA reveals a distinctive ligand-activated transcription factor. *Proc Natl Acad Sci U S A* 89:8185-8189.
22. Wang, G.L., Jiang, B.H., Rue, E.A., and Semenza, G.L. 1995. Hypoxia-inducible factor 1 is a basic-helix-loop-helix-PAS heterodimer regulated by cellular O₂ tension. *Proc Natl Acad Sci U S A* 92:5510-5514.
23. Forsythe, J.A., Jiang, B.H., Iyer, N.V., Agani, F., Leung, S.W., Koos, R.D., and Semenza, G.L. 1996. Activation of vascular endothelial growth factor gene transcription by hypoxia-inducible factor 1. *Mol Cell Biol* 16:4604-4613.
24. Maltepe, E., Schmidt, J.V., Baunoch, D., Bradfield, C.A., and Simon, M.C. 1997. Abnormal angiogenesis and responses to glucose and oxygen deprivation in mice lacking the protein ARNT. *Nature* 386:403-407.
25. Kotch, L.E., Iyer, N.V., Laughner, E., and Semenza, G.L. 1999. Defective vascularization of HIF-1alpha-null embryos is not associated with VEGF deficiency but with mesenchymal cell death. *Dev Biol* 209:254-267.
26. Folkman, J., and Shing, Y. 1992. Angiogenesis. *J Biol Chem* 267:10931-10934.
27. Alon, T., Hemo, I., Itin, A., Pe'er, J., Stone, J., and Keshet, E. 1995. Vascular endothelial growth factor acts as a survival factor for newly formed retinal vessels and has implications for retinopathy of prematurity. *Nat Med* 1:1024-1028.
28. Munoz-Chapuli, R., Quesada, A.R., and Angel Medina, M. 2004. Angiogenesis and signal transduction in endothelial cells. *Cell Mol Life Sci* 61:2224-2243.

29. Keck, P.J., Hauser, S.D., Krivi, G., Sanzo, K., Warren, T., Feder, J., and Connolly, D.T. 1989. Vascular permeability factor, an endothelial cell mitogen related to PDGF. *Science* 246:1309-1312.
30. Jain, R.K. 2003. Molecular regulation of vessel maturation. *Nat Med* 9:685-693.
31. Sato, T.N., Tozawa, Y., Deutsch, U., Wolburg-Buchholz, K., Fujiwara, Y., Gendron-Maguire, M., Gridley, T., Wolburg, H., Risau, W., and Qin, Y. 1995. Distinct roles of the receptor tyrosine kinases Tie-1 and Tie-2 in blood vessel formation. *Nature* 376:70-74.
32. Gittenberger-de Groot, A.C., DeRuiter, M.C., Bergwerff, M., and Poelmann, R.E. 1999. Smooth muscle cell origin and its relation to heterogeneity in development and disease. *Arterioscler Thromb Vasc Biol* 19:1589-1594.
33. Hungerford, J.E., and Little, C.D. 1999. Developmental biology of the vascular smooth muscle cell: building a multilayered vessel wall. *J Vasc Res* 36:2-27.
34. Hirschi, K.K., Rohovsky, S.A., and D'Amore, P.A. 1998. PDGF, TGF-beta, and heterotypic cell-cell interactions mediate endothelial cell-induced recruitment of 10T1/2 cells and their differentiation to a smooth muscle fate. *J Cell Biol* 141:805-814.
35. Hirschi, K.K., Rohovsky, S.A., Beck, L.H., Smith, S.R., and D'Amore, P.A. 1999. Endothelial cells modulate the proliferation of mural cell precursors via platelet-derived growth factor-BB and heterotypic cell contact. *Circ Res* 84:298-305.
36. Berk, B.C. 2001. Vascular smooth muscle growth: autocrine growth mechanisms. *Physiol Rev* 81:999-1030.
37. Le Lievre, C.S., and Le Douarin, N.M. 1975. Mesenchymal derivatives of the neural crest: analysis of chimaeric quail and chick embryos. *J Embryol Exp Morphol* 34:125-154.
38. Bergwerff, M., Verberne, M.E., DeRuiter, M.C., Poelmann, R.E., and Gittenberger-de Groot, A.C. 1998. Neural crest cell contribution to the developing circulatory system: implications for vascular morphology? *Circ Res* 82:221-231.
39. Rosenquist, T.H., and Beall, A.C. 1990. Elastogenic cells in the developing cardiovascular system. Smooth muscle, nonmuscle, and cardiac neural crest. *Ann N Y Acad Sci* 588:106-119.
40. Saint-Jeannet, J.P., Levi, G., Girault, J.M., Koteliansky, V., and Thiery, J.P. 1992. Ventrolateral regionalization of *Xenopus laevis* mesoderm is characterized by the expression of alpha-smooth muscle actin. *Development* 115:1165-1173.
41. Hungerford, J.E., Owens, G.K., Argraves, W.S., and Little, C.D. 1996. Development of the aortic vessel wall as defined by vascular smooth muscle and extracellular matrix markers. *Dev Biol* 178:375-392.
42. Vrancken Peeters, M.P., Gittenberger-de Groot, A.C., Mentink, M.M., and Poelmann, R.E. 1999. Smooth muscle cells and fibroblasts of the coronary arteries derive from epithelial-mesenchymal transformation of the epicardium. *Anat Embryol (Berl)* 199:367-378.

43. Dettman, R.W., Denetclaw, W., Jr., Ordahl, C.P., and Bristow, J. 1998. Common epicardial origin of coronary vascular smooth muscle, perivascular fibroblasts, and intermyocardial fibroblasts in the avian heart. *Dev Biol* 193:169-181.
44. DeRuiter, M.C., Poelmann, R.E., VanMunsteren, J.C., Mironov, V., Markwald, R.R., and Gittenberger-de Groot, A.C. 1997. Embryonic endothelial cells transdifferentiate into mesenchymal cells expressing smooth muscle actins in vivo and in vitro. *Circ Res* 80:444-451.
45. Arciniegas, E., Sutton, A.B., Allen, T.D., and Schor, A.M. 1992. Transforming growth factor beta 1 promotes the differentiation of endothelial cells into smooth muscle-like cells in vitro. *J Cell Sci* 103 (Pt 2):521-529.
46. Suri, C., Jones, P.F., Patan, S., Bartunkova, S., Maisonpierre, P.C., Davis, S., Sato, T.N., and Yancopoulos, G.D. 1996. Requisite role of angiopoietin-1, a ligand for the TIE2 receptor, during embryonic angiogenesis. *Cell* 87:1171-1180.
47. Kuo, C.T., Veselits, M.L., Barton, K.P., Lu, M.M., Clendenin, C., and Leiden, J.M. 1997. The LKLF transcription factor is required for normal tunica media formation and blood vessel stabilization during murine embryogenesis. *Genes Dev* 11:2996-3006.
48. Adams, R.H., Diella, F., Hennig, S., Helmbacher, F., Deutsch, U., and Klein, R. 2001. The cytoplasmic domain of the ligand ephrinB2 is required for vascular morphogenesis but not cranial neural crest migration. *Cell* 104:57-69.
49. ten Dijke, P., and Hill, C.S. 2004. New insights into TGF-beta-Smad signalling. *Trends Biochem Sci* 29:265-273.
50. Moustakas, A., Souchelnytskyi, S., and Heldin, C.H. 2001. Smad regulation in TGF-beta signal transduction. *J Cell Sci* 114:4359-4369.
51. Yang, X., Castilla, L.H., Xu, X., Li, C., Gotay, J., Weinstein, M., Liu, P.P., and Deng, C.X. 1999. Angiogenesis defects and mesenchymal apoptosis in mice lacking SMAD5. *Development* 126:1571-1580.
52. Yamagishi, H., Olson, E.N., and Srivastava, D. 2000. The basic helix-loop-helix transcription factor, dHAND, is required for vascular development. *J Clin Invest* 105:261-270.
53. Kappel, A., Schlaeger, T.M., Flamme, I., Orkin, S.H., Risau, W., and Breier, G. 2000. Role of SCL/Tal-1, GATA, and ets transcription factor binding sites for the regulation of flk-1 expression during murine vascular development. *Blood* 96:3078-3085.
54. Wakiya, K., Begue, A., Stehelin, D., and Shibuya, M. 1996. A cAMP response element and an Ets motif are involved in the transcriptional regulation of flt-1 tyrosine kinase (vascular endothelial growth factor receptor 1) gene. *J Biol Chem* 271:30823-30828.
55. Dube, A., Akbarali, Y., Sato, T.N., Libermann, T.A., and Oettgen, P. 1999. Role of the Ets transcription factors in the regulation of the vascular-specific Tie2 gene. *Circ Res* 84:1177-1185.

56. Iljin, K., Dube, A., Kontusaari, S., Korhonen, J., Lahtinen, I., Oettgen, P., and Alitalo, K. 1999. Role of ets factors in the activity and endothelial cell specificity of the mouse Tie gene promoter. *Faseb J* 13:377-386.
57. Lin, Q., Lu, J., Yanagisawa, H., Webb, R., Lyons, G.E., Richardson, J.A., and Olson, E.N. 1998. Requirement of the MADS-box transcription factor MEF2C for vascular development. *Development* 125:4565-4574.
58. Bi, W., Drake, C.J., and Schwarz, J.J. 1999. The transcription factor MEF2C-null mouse exhibits complex vascular malformations and reduced cardiac expression of angiopoietin 1 and VEGF. *Dev Biol* 211:255-267.
59. Black, B.L., and Olson, E.N. 1998. Transcriptional control of muscle development by myocyte enhancer factor-2 (MEF2) proteins. *Annu Rev Cell Dev Biol* 14:167-196.
60. Olson, E.N., Perry, M., and Schulz, R.A. 1995. Regulation of muscle differentiation by the MEF2 family of MADS box transcription factors. *Dev Biol* 172:2-14.
61. Molkentin, J.D., Black, B.L., Martin, J.F., and Olson, E.N. 1995. Cooperative activation of muscle gene expression by MEF2 and myogenic bHLH proteins. *Cell* 83:1125-1136.
62. Black, B.L., Molkentin, J.D., and Olson, E.N. 1998. Multiple roles for the MyoD basic region in transmission of transcriptional activation signals and interaction with MEF2. *Mol Cell Biol* 18:69-77.
63. Fickett, J.W. 1996. Coordinate positioning of MEF2 and myogenin binding sites. *Gene* 172:GC19-32.
64. Edmondson, D.G., Lyons, G.E., Martin, J.F., and Olson, E.N. 1994. Mef2 gene expression marks the cardiac and skeletal muscle lineages during mouse embryogenesis. *Development* 120:1251-1263.
65. Subramanian, S.V., and Nadal-Ginard, B. 1996. Early expression of the different isoforms of the myocyte enhancer factor-2 (MEF2) protein in myogenic as well as non-myogenic cell lineages during mouse embryogenesis. *Mech Dev* 57:103-112.
66. Leifer, D., Krainc, D., Yu, Y.T., McDermott, J., Breitbart, R.E., Heng, J., Neve, R.L., Kosofsky, B., Nadal-Ginard, B., and Lipton, S.A. 1993. MEF2C, a MADS/MEF2-family transcription factor expressed in a laminar distribution in cerebral cortex. *Proc Natl Acad Sci U S A* 90:1546-1550.
67. Lyons, G.E., Micales, B.K., Schwarz, J., Martin, J.F., and Olson, E.N. 1995. Expression of mef2 genes in the mouse central nervous system suggests a role in neuronal maturation. *J Neurosci* 15:5727-5738.
68. Swanson, B.J., Jack, H.M., and Lyons, G.E. 1998. Characterization of myocyte enhancer factor 2 (MEF2) expression in B and T cells: MEF2C is a B cell-restricted transcription factor in lymphocytes. *Mol Immunol* 35:445-458.
69. Hofmann, S.L., Brown, M.S., Lee, E., Pathak, R.K., Anderson, R.G., and Goldstein, J.L. 1989. Purification of a sarcoplasmic reticulum protein that binds Ca²⁺ and plasma lipoproteins. *J Biol Chem* 264:8260-8270.

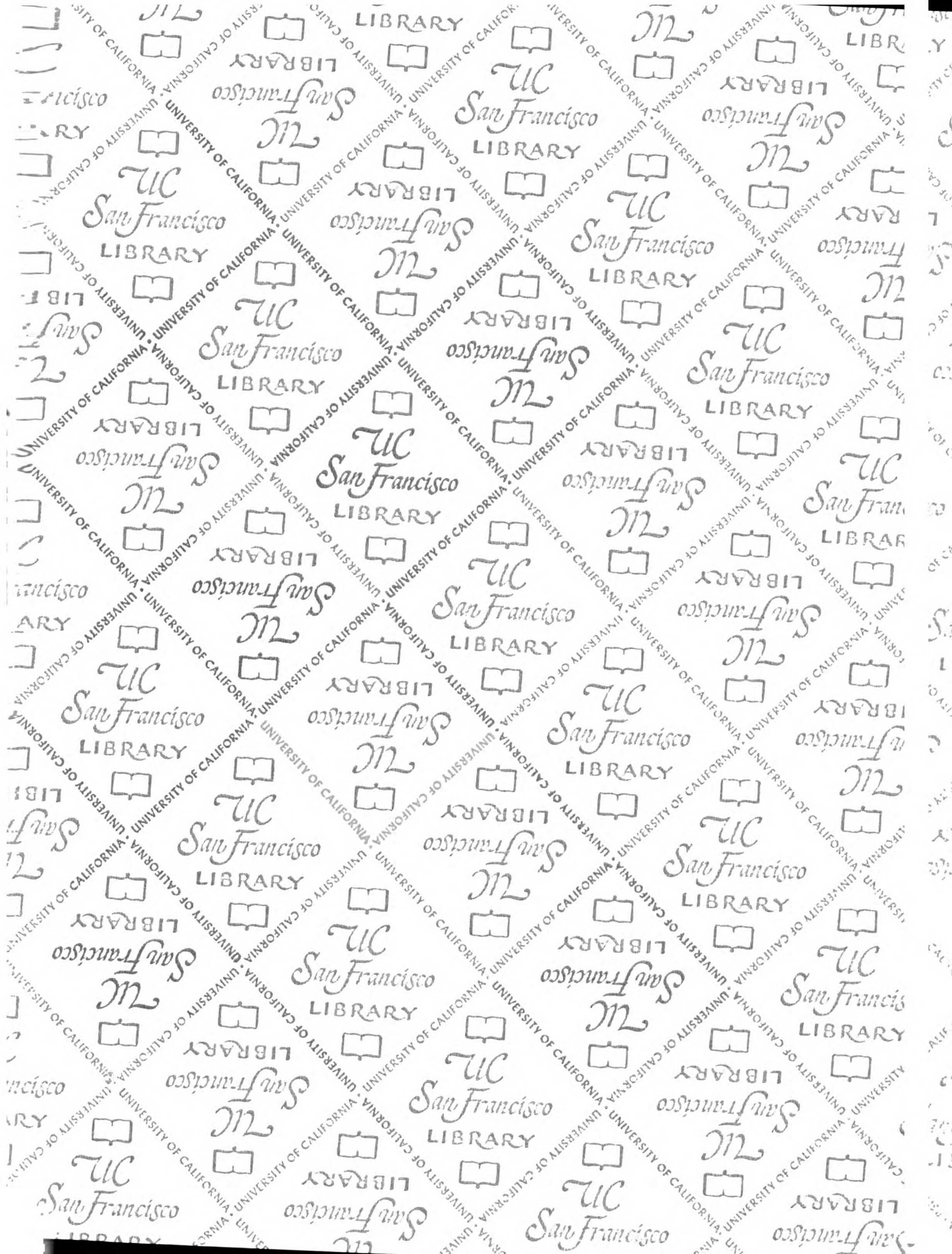
70. Hofmann, S.L., Goldstein, J.L., Orth, K., Moomaw, C.R., Slaughter, C.A., and Brown, M.S. 1989. Molecular cloning of a histidine-rich Ca²⁺-binding protein of sarcoplasmic reticulum that contains highly conserved repeated elements. *J Biol Chem* 264:18083-18090.
71. Pathak, R.K., Anderson, R.G., and Hofmann, S.L. 1992. Histidine-rich calcium binding protein, a sarcoplasmic reticulum protein of striated muscle, is also abundant in arteriolar smooth muscle cells. *J Muscle Res Cell Motil* 13:366-376.
72. Damiani, E., and Margreth, A. 1991. Subcellular fractionation to junctional sarcoplasmic reticulum and biochemical characterization of 170 kDa Ca(2+)- and low-density-lipoprotein-binding protein in rabbit skeletal muscle. *Biochem J* 277 (Pt 3):825-832.
73. Lee, H.G., Kang, H., Kim, D.H., and Park, W.J. 2001. Interaction of HRC (histidine-rich Ca(2+)-binding protein) and triadin in the lumen of sarcoplasmic reticulum. *J Biol Chem* 276:39533-39538.
74. Suk, J.Y., Kim, Y.S., and Park, W.J. 1999. HRC (histidine-rich Ca²⁺ binding protein) resides in the lumen of sarcoplasmic reticulum as a multimer. *Biochem Biophys Res Commun* 263:667-671.
75. Picello, E., Damiani, E., and Margreth, A. 1992. Low-affinity Ca(2+)-binding sites versus Zn(2+)-binding sites in histidine-rich Ca(2+)-binding protein of skeletal muscle sarcoplasmic reticulum. *Biochem Biophys Res Commun* 186:659-667.
76. Kim, E., Shin, D.W., Hong, C.S., Jeong, D., Kim do, H., and Park, W.J. 2003. Increased Ca²⁺ storage capacity in the sarcoplasmic reticulum by overexpression of HRC (histidine-rich Ca²⁺ binding protein). *Biochem Biophys Res Commun* 300:192-196.
77. Parmacek, M.S. 2001. Transcriptional programs regulating vascular smooth muscle cell development and differentiation. *Curr Top Dev Biol* 51:69-89.
78. Chang, Y.F., Wei, J., Liu, X., Chen, Y.H., Layne, M.D., and Yet, S.F. 2003. Identification of a CARG-independent region of the cysteine-rich protein 2 promoter that directs expression in the developing vasculature. *Am J Physiol Heart Circ Physiol* 285:H1675-1683.
79. Layne, M.D., Yet, S.F., Maemura, K., Hsieh, C.M., Liu, X., Ith, B., Lee, M.E., and Perrella, M.A. 2002. Characterization of the mouse aortic carboxypeptidase-like protein promoter reveals activity in differentiated and dedifferentiated vascular smooth muscle cells. *Circ Res* 90:728-736.
80. Cheng, T.C., Wallace, M.C., Merlie, J.P., and Olson, E.N. 1993. Separable regulatory elements governing myogenin transcription in mouse embryogenesis. *Science* 261:215-218.
81. Edmondson, D.G., Cheng, T.C., Cserjesi, P., Chakraborty, T., and Olson, E.N. 1992. Analysis of the myogenin promoter reveals an indirect pathway for positive autoregulation mediated by the muscle-specific enhancer factor MEF-2. *Mol Cell Biol* 12:3665-3677.

82. Yee, S.P., and Rigby, P.W. 1993. The regulation of myogenin gene expression during the embryonic development of the mouse. *Genes Dev* 7:1277-1289.
83. Hogan. 1994. *Manipulating the Mouse Embryo*. Plainview, NY: Cold Spring Harbor Laboratory Press.
84. Rishniw, M., Xin, H.B., Deng, K.Y., and Kotlikoff, M.I. 2003. Skeletal myogenesis in the mouse esophagus does not occur through transdifferentiation. *Genesis* 36:81-82.
85. McKinsey, T.A., Zhang, C.L., and Olson, E.N. 2001. Control of muscle development by dueling HATs and HDACs. *Curr Opin Genet Dev* 11:497-504.
86. Lu, J., McKinsey, T.A., Zhang, C.L., and Olson, E.N. 2000. Regulation of skeletal myogenesis by association of the MEF2 transcription factor with class II histone deacetylases. *Mol Cell* 6:233-244.
87. McKinsey, T.A., Zhang, C.L., Lu, J., and Olson, E.N. 2000. Signal-dependent nuclear export of a histone deacetylase regulates muscle differentiation. *Nature* 408:106-111.
88. Grozinger, C.M., and Schreiber, S.L. 2000. Regulation of histone deacetylase 4 and 5 and transcriptional activity by 14-3-3-dependent cellular localization. *Proc Natl Acad Sci U S A* 97:7835-7840.
89. Wang, A.H., Kruhlak, M.J., Wu, J., Bertos, N.R., Vezmar, M., Posner, B.I., Bazett-Jones, D.P., and Yang, X.J. 2000. Regulation of histone deacetylase 4 by binding of 14-3-3 proteins. *Mol Cell Biol* 20:6904-6912.
90. McKinsey, T.A., Zhang, C.L., and Olson, E.N. 2000. Activation of the myocyte enhancer factor-2 transcription factor by calcium/calmodulin-dependent protein kinase-stimulated binding of 14-3-3 to histone deacetylase 5. *Proc Natl Acad Sci U S A* 97:14400-14405.
91. Morin, S., Charron, F., Robitaille, L., and Nemer, M. 2000. GATA-dependent recruitment of MEF2 proteins to target promoters. *Embo J* 19:2046-2055.
92. Chang, D.F., Belaguli, N.S., Iyer, D., Roberts, W.B., Wu, S.P., Dong, X.R., Marx, J.G., Moore, M.S., Beckerle, M.C., Majesky, M.W., et al. 2003. Cysteine-rich LIM-only proteins CRP1 and CRP2 are potent smooth muscle differentiation cofactors. *Dev Cell* 4:107-118.
93. Dodou, E., Verzi, M.P., Anderson, J.P., Xu, S.M., and Black, B.L. 2004. Mef2c is a direct transcriptional target of ISL1 and GATA factors in the anterior heart field during mouse embryonic development. *Development* 131:3931-3942.
94. Kothary, R., Clapoff, S., Darling, S., Perry, M.D., Moran, L.A., and Rossant, J. 1989. Inducible expression of an hsp68-lacZ hybrid gene in transgenic mice. *Development* 105:707-714.
95. Dodou, E., Xu, S.M., and Black, B.L. 2003. mef2c is activated directly by myogenic basic helix-loop-helix proteins during skeletal muscle development in vivo. *Mech Dev* 120:1021-1032.

96. De Val, S., Anderson, J.P., Heidt, A.B., Khiem, D., Xu, S.M., and Black, B.L. 2004. Mef2c is activated directly by Ets transcription factors through an evolutionarily conserved endothelial cell-specific enhancer. *Dev Biol* 275:424-434.
97. Lelievre, E., Lionneton, F., Soncin, F., and Vandebunder, B. 2001. The Ets family contains transcriptional activators and repressors involved in angiogenesis. *Int J Biochem Cell Biol* 33:391-407.
98. Nye, J.A., Petersen, J.M., Gunther, C.V., Jonsen, M.D., and Graves, B.J. 1992. Interaction of murine ets-1 with GGA-binding sites establishes the ETS domain as a new DNA-binding motif. *Genes Dev* 6:975-990.
99. Sharrocks, A.D., Brown, A.L., Ling, Y., and Yates, P.R. 1997. The ETS-domain transcription factor family. *Int J Biochem Cell Biol* 29:1371-1387.
100. Wang, C.Y., Petryniak, B., Ho, I.C., Thompson, C.B., and Leiden, J.M. 1992. Evolutionarily conserved Ets family members display distinct DNA binding specificities. *J Exp Med* 175:1391-1399.
101. Shore, P., and Sharrocks, A.D. 1995. The ETS-domain transcription factors Elk-1 and SAP-1 exhibit differential DNA binding specificities. *Nucleic Acids Res* 23:4698-4706.
102. Sharrocks, A.D. 2001. The ETS-domain transcription factor family. *Nat Rev Mol Cell Biol* 2:827-837.
103. Consales, C., and Arnone, M.I. 2002. Functional characterization of Ets-binding sites in the sea urchin embryo: three base pair conversions redirect expression from mesoderm to ectoderm and endoderm. *Gene* 287:75-81.
104. Serbedzija, G.N., and McMahon, A.P. 1997. Analysis of neural crest cell migration in Splotch mice using a neural crest-specific LacZ reporter. *Dev Biol* 185:139-147.
105. Pusch, C., Hustert, E., Pfeifer, D., Sudbeck, P., Kist, R., Roe, B., Wang, Z., Balling, R., Blin, N., and Scherer, G. 1998. The SOX10/Sox10 gene from human and mouse: sequence, expression, and transactivation by the encoded HMG domain transcription factor. *Hum Genet* 103:115-123.
106. Pietri, T., Eder, O., Blanche, M., Thiery, J.P., and Dufour, S. 2003. The human tissue plasminogen activator-Cre mouse: a new tool for targeting specifically neural crest cells and their derivatives in vivo. *Dev Biol* 259:176-187.
107. Chin, E.R., Olson, E.N., Richardson, J.A., Yang, Q., Humphries, C., Shelton, J.M., Wu, H., Zhu, W., Bassel-Duby, R., and Williams, R.S. 1998. A calcineurin-dependent transcriptional pathway controls skeletal muscle fiber type. *Genes Dev* 12:2499-2509.
108. Stevenson, A.S., Gomez, M.F., Hill-Eubanks, D.C., and Nelson, M.T. 2001. NFAT4 movement in native smooth muscle. A role for differential Ca(2+) signaling. *J Biol Chem* 276:15018-15024.
109. Dave, V., Childs, T., and Whitsett, J.A. 2004. Nuclear factor of activated T cells regulates transcription of the surfactant protein D gene (Sftpd) via direct

- interaction with thyroid transcription factor-1 in lung epithelial cells. *J Biol Chem* 279:34578-34588.
110. Chang, C.P., Neilson, J.R., Bayle, J.H., Gestwicki, J.E., Kuo, A., Stankunas, K., Graef, I.A., and Crabtree, G.R. 2004. A field of myocardial-endocardial NFAT signaling underlies heart valve morphogenesis. *Cell* 118:649-663.
 111. Cockerill, G.W., Bert, A.G., Ryan, G.R., Gamble, J.R., Vadas, M.A., and Cockerill, P.N. 1995. Regulation of granulocyte-macrophage colony-stimulating factor and E-selectin expression in endothelial cells by cyclosporin A and the T-cell transcription factor NFAT. *Blood* 86:2689-2698.
 112. Kabrun, N., Buhring, H.J., Choi, K., Ullrich, A., Risau, W., and Keller, G. 1997. Flk-1 expression defines a population of early embryonic hematopoietic precursors. *Development* 124:2039-2048.
 113. Wasylyk, C., Gutman, A., Nicholson, R., and Wasylyk, B. 1991. The c-Ets oncoprotein activates the stromelysin promoter through the same elements as several non-nuclear oncoproteins. *Embo J* 10:1127-1134.
 114. Li, L., Miano, J.M., Mercer, B., and Olson, E.N. 1996. Expression of the SM22alpha promoter in transgenic mice provides evidence for distinct transcriptional regulatory programs in vascular and visceral smooth muscle cells. *J Cell Biol* 132:849-859.
 115. Li, L., Liu, Z., Mercer, B., Overbeek, P., and Olson, E.N. 1997. Evidence for serum response factor-mediated regulatory networks governing SM22alpha transcription in smooth, skeletal, and cardiac muscle cells. *Dev Biol* 187:311-321.
 116. Mack, C.P., and Owens, G.K. 1999. Regulation of smooth muscle alpha-actin expression in vivo is dependent on CARG elements within the 5' and first intron promoter regions. *Circ Res* 84:852-861.
 117. Mack, C.P., Thompson, M.M., Lawrenz-Smith, S., and Owens, G.K. 2000. Smooth muscle alpha-actin CARG elements coordinate formation of a smooth muscle cell-selective, serum response factor-containing activation complex. *Circ Res* 86:221-232.
 118. McFadden, D.G., Charite, J., Richardson, J.A., Srivastava, D., Firulli, A.B., and Olson, E.N. 2000. A GATA-dependent right ventricular enhancer controls dHAND transcription in the developing heart. *Development* 127:5331-5341.
 119. Black, B.L., Martin, J.F., and Olson, E.N. 1995. The mouse MRF4 promoter is trans-activated directly and indirectly by muscle-specific transcription factors. *J Biol Chem* 270:2889-2892.
 120. Wang, D.Z., Li, S., Hockemeyer, D., Sutherland, L., Wang, Z., Schrott, G., Richardson, J.A., Nordheim, A., and Olson, E.N. 2002. Potentiation of serum response factor activity by a family of myocardin-related transcription factors. *Proc Natl Acad Sci U S A* 99:14855-14860.
 121. Horton, R.M. 1997. *SOEing Together Tailor-Made Genes*. Totowa, NJ: Humana Press. 141-149 pp.

122. Black, B.L., Lu, J., and Olson, E.N. 1997. The MEF2A 3' untranslated region functions as a cis-acting translational repressor. *Mol Cell Biol* 17:2756-2763.
123. Cripps, R.M., Black, B.L., Zhao, B., Lien, C.L., Schulz, R.A., and Olson, E.N. 1998. The myogenic regulatory gene Mef2 is a direct target for transcriptional activation by Twist during *Drosophila* myogenesis. *Genes Dev* 12:422-434.
124. Verzi, M.P., Anderson, J.P., Dodou, E., Kelly, K.K., Greene, S.B., North, B.J., Cripps, R.M., and Black, B.L. 2002. N-twist, an evolutionarily conserved bHLH protein expressed in the developing CNS, functions as a transcriptional inhibitor. *Dev Biol* 249:174-190.



For reference

Not to be taken
from the room.

8070685



3 1378 00807 0685

